Western Norway University of Applied Sciences

BACHELOR'S ASSIGNMENT

Fluorometry investigations of the hydrology at the Skjerdingane glacier

Fluorometriundersøkelser av hydrologien ved Skjerdinganebreen

Geology and geohazards

GE491

AIN

01.06.2017

Number of words: 17 238

ANDERS HALSNES AND JAN HEDGES

Supervisor: Simon de Villiers

I confirm that the work is self-prepared and that references/source references to all sources used in the work are provided, *cf. Regulation relating to academic studies and examinations at the Western Norway University of Applied Sciences (HVL), § 10*

Abstract

Alpine cirque glaciers and their drainage systems are difficult to access and study, but they represent an important part of the glaciated surface in alpine regions. A better understanding of the hydrology of alpine cirque glaciers may offer valuable insights about the glacier itself, the surrounding macro- and microclimates, and how these are interrelated and change over time. Fluorometric dye tracing techniques have been used extensively to study these remote systems. The Skjerdingane glacier in Sogndalsdalen in southern Norway is a cirque glacier which is located below its climatological equilibrium line, which makes it a particularly interesting glacier to study.

The project aim is to determine the suitability of using fluorometry techniques to study the englacial and proglacial drainage systems of the Skjerdingane cirque glacier. A substantial part of our investigation is focused on understanding the methods used in dye tracing, by approaching the methods from different angles.

In this thesis, we use dye tracing to measure the discharge of the proglacial stream originating at the Skjerdingane glacier during melting season. We have also performed several measurements on the englacial drainage system, which proved difficult due to the presence of a glacial lake. Based on this, we did a preliminary investigation into the problems associated with passing dye signals through large bodies of standing water.

These results were accomplished through studying fluorometry techniques at three different levels; 1) simulating the diffusion of dye with a numerical model, 2) experimenting with different dye tracing setups in the laboratory, and 3) combining these findings with our field measurements from the Skjerdingane glacier.

Table of contents

1 Introduction 1
1.1 Outline of thesis 2
1.2 Research question 2
1.3 Field location 3

2 Theoretical background 5
2.1 Numerical model 5
2.1.1 Modelling diffusion in one dimension 5
2.1.2 Altering the diffusion equation 5
2.1.3 Introducing movement in the model 6
2.1.4 Applications of the model 7
2.2 Dye tracing theory 7
2.2.1 Fluorescent dyes 7
2.2.2 Parameters which affect the fluorescence of dyes 8
2.2.3 Slug injection and discharge measurements 9
2.2.4 Breakthrough curve analysis 10
2.2.5 Dye dispersion 11

3 Methods and experimental setup 13
3.1 Numerical modelling 13
3.1.1 Setting up the numerical model in excel 13
3.1.2 Defining Dirichlet boundary conditions 14
3.1.3 Modelling diffusion in still standing water 15
3.1.4 Modelling dispersion in moving water 16
3.2 Dye tracing techniques 17
3.2.1 Rhodamine WT 17
3.2.2 The fluorometer: Cyclops 7 and DataBank 17
3.2.3 Dye measuring and dye injection methods 19
3.2.4 Calibration procedure 19
3.2.5 Concentration calculations 20
3.2.6 Lab calibration 20
3.2.7 Field calibration 21
3.2.8 Accounting for temperature changes 22
3.2.9 Generating the mV to concentration equations 22
3.3 Lab methods 23
3.3.1 Diffusion experiment setup 23
3.3.2 Siphon experiment setup 24
3.3.1 Stream and basin experiment setup 26
3.4 Fieldwork 28
3.4.1 Overview 28
3.4.2 Field map 29
3.4.3 Using the fluorometer in the field 29
3.4.4 Glacier measurements set up 30
3.4.5 Stream and valley lake measurements set up 31
3.4.6 Supraglacial stream and glacial lake set up 32

4 Results and analysis 34
4.1 Diffusion 34
A - Results 34
B – Analysis 35
4.2 Lab experiments 36
4.2.1 Lab calibration results 36
4.2.2 Siphon experiment results and analysis 37
4.2.3 Stream and basin experiment results and analysis 38

4.3 Field results 39
4.3.1 Field calibration results *39*
4.3.2 Proglacial stream measurement *40*
4.3.3 Valley lake measurement *41*
4.3.4 Glacier measurements *41*
A - Results *41*
B - Analysis *43*
4.3.5 Supraglacial stream and glacial lake measurements *43*
A - Results *43*
B - Analysis and discussion *44*
4.4 Numerical modelling results 46
A - Results *46*
B – Analysis *48*
5 Discussion 49
5.1 Numerical modelling 49
5.1.1 Model reliability *49*
5.1.2 Use of the model *50*
5.1.3 Further model investigations *50*
5.2 Stream discharge measurements 51
5.2.1 Test of reliability in lab *51*
5.2.2 Estimates of field discharge in the proglacial stream in Skjerdingane *52*
5.2.3 Discussion of error sources *52*
5.2.4 Suggestions for improved discharge estimates *53*
5.3 Lack of signal in glacier measurements 53
5.3.1 Glacier #2 ..... *53*
5.3.2 Glacier #3 ..... *54*
5.3.3 Effects of the glacial lake *55*
5.3.4 Further investigations *55*
5.4 Effects of passing dye signals through large water volumes 56
5.4.1 Test of signal reduction in the lab *56*
5.4.2 Valley lake signal distortion *57*
5.4.3 Glacier lake signal distortion *57*
5.4.4 Temperature effects *60*
5.4.5 Error sources *60*
5.4.6 Further investigations *60*
6 Conclusion 62
7 References 63

List of equations

(1) $\frac{\partial u}{\partial t} = \alpha^2 \frac{\partial^2 u}{\partial x^2}$

(2) $\frac{\partial u}{\partial t}(x,t) = \frac{u(x,t+\Delta t)-u(x,t)}{\Delta t}$

(3) $\frac{\partial^2 u}{\partial x^2}(x,t) = \frac{u(x+\Delta x,t)-2u(x,t)+u(x-\Delta x,t)}{\Delta x^2}$

(4) $\frac{u(x,t+\Delta t)-u(x,t)}{\Delta t} = D\,\frac{u(x+\Delta x,t)-2u(x,t)+u(x-\Delta x,t)}{\Delta x^2}$

(5) $u(x,t+\Delta t) = u(x,t) + K\{u(x+\Delta x,t) - 2u(x,t) + u(x-\Delta x,t)\}$

(6) $K = D\left(\frac{\Delta t}{\Delta x^2}\right)$

(7) $u_x^{t+1} = (u-1) + \frac{u-(u-1)}{\Delta x}\Delta x v$

(8) $D_{T0} = D_T e^{0.027(T-T0)}$

(9) $Q = \frac{M}{A_c}$

(10) $u = \frac{d}{t_m}$

(11) $Q = \frac{S_g V_i C}{A_c}$

(12) $A_{sm} = \frac{Q}{u}$

(13) $Re = \frac{QR_H}{vA}$

(14) $D = \frac{d^2(t_m-t_i)^2}{4t_m^2 t_i ln\left[2\left(\frac{t_m}{t_i}\right)^{\frac{1}{2}}\right]}$

(15) $D = \alpha u \quad \rightarrow \quad \alpha = \frac{D}{u}$

(16) $u_n^{k+1} = u_n^k + K(u_{n+1}^k - 2u_n^k + u_{n-1}^k)$

(17) $u_n^{k+1} = u_n^k + K\left(u_{n+1}^k - 2u_n^k + u_{n-1}^k\right) + \left[u_{n-1}^{k+1} + \frac{u_n^{k+1}-(u_{n-1}^{k+1})}{\Delta x}\Delta x v\right]$

(18) $C_{(1)} = \frac{S_{g(d)} V_{i(1)} C_{(d)}}{V_{w(1)}}$

(19) $C_{(2)} = \frac{S_{g(1)} V_{i(2)} C_{(1)}}{V_{w(2)}}$

(20) $C_{(2)} = \frac{V_{i(1)} V_{i(2)} S_{g(d)} C_{(d)}}{V_w(1) V_w(2)}$

1 Introduction

A better understanding of the properties of glaciers and their hydrology, and how these change in response to climatic changes, is important in the ongoing debate regarding global climate change. To investigate the subglacial drainage system of glaciers, which are not easily accessible, tracer studies using fluorometric dyes have been used (Fountain, 1993; Willis, Sharp, & Richards, 1990). Using tracer studies, it is possible to estimate several parameters of interest from the glaciers hydrological system (Fyffe, 2013).

In our project, we have applied fluorometric dye tracing techniques to investigate the hydrology of the Skjerdingane cirque glacier. Similar investigations have been performed on Storglaciären (Seaberg, Seaberg, Hooke, & Wiberg, 1988), Midtdalsbreen (Willis et al., 1990) and Storbrean (Hubbard & Glasser, 2005), to mention a few regional examples.

After development of new fluorescent dyes and fluorometers in the 1960s, the techniques used in fluorometric dye tracing were thoroughly described (Wilson, Cobb, & Kilpatrick, 1968) and the properties of the different dye types were studied (Smart & Laidlaw, 1977). These dye tracing techniques have been applied to measurements of discharge (Kilpatrick & Cobb, 1985) and investigations on glacier hydrology (Fyffe, 2013). Others have focused on the losses of dye to sorption onto sediments (Bencala et al., 1983) and the effects of channel properties on dye traces (Gulley et al., 2012).

In our work, we have applied a three-step approach. Simulations, lab experiments and field measurements have been combined to increase our understanding of the methods behind fluorometric dye tracing. Estimates of the meltwater discharge from the Skjerdingane glacier have been made at two occasions during the melting season of 2016. Investigations have also been made into the subglacial drainage system of the glacier. Through numerical modelling, lab experiments and a combination of these with the field measurements, we have performed a general investigation into fluorometric dye tracing techniques. Our dye injections at back of the glacier did not return detectable fluorescence measurements. Because of this, the investigation has been partially focused on the effect of passing a dye signal through a large body of standing water. Using both lab experiments and field measurements, we have attempted to quantify the amount of dye required to sufficiently preserve the dye signal through a water volume in a given hydraulic system.

1.1 Outline of thesis

The three distinct levels of approach; modelling, experiments and measurements, are present throughout the thesis. In section 2, we go through the theoretical background for our numerical model, as well as the dye tracing theory behind our lab experiments and field measurements. Similarly, section 3 on methods first describes how our numerical model has been designed, then how the lab experiments were set up and finally how the field measurements were carried out. In section 4, results and analysis, we present our results from simulations, lab experiments and field measurements along with a short analysis. A discussion of the results is presented in section 5, and a conclusion is given in section 6.

1.2 Research question

How can we use theoretical simulations and empirical lab experiments to better interpret actual fluorometry measurements from the hydrological system of the Skjerdingane cirque glacier?

To answer this, we will look at;

- How can we use our numerical model to better understand the impact different variables have on the diffusion and dispersion of dyes?
- How good is our numerical model at simulating breakthrough curves and predicting dye trace parameters like dispersion?
- How good is our fluorometric dye tracing method at predicting discharge during controlled lab experiments?
- How is a breakthrough curve affected when it is passed through a large water volume?

1.3 Field location

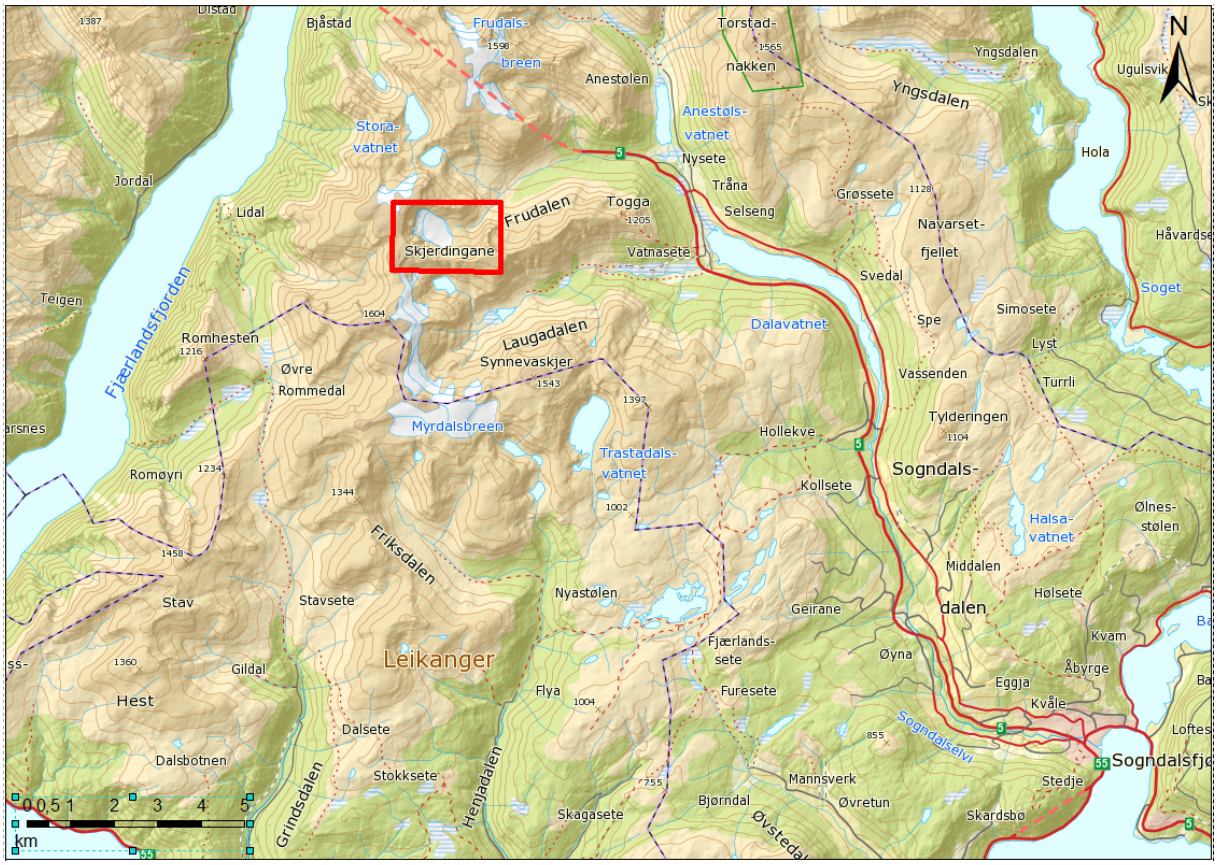

Figure 1.1 A map of Sogndalsdalen in Sogn og Fjordane. The red square highlights the location of the Skjerdingane cirque glacier. Field work was carried out on the glacier and in the hanging valley directly below it. (Kartverket)

The location for our field work was the Skjerdingane cirque glacier, and the proglacial stream from its meltwater. The glacier is situated in the western end of Frudalen, Sogn og Fjordane, Norway shown in figure 1.1 and figure 1.2. The glacier is situated in an east facing cirque, with steep mountainsides surrounding it. The highest point on the glacier is at about 1205 meters above sea level (m a.s.l). It glacier has its lowest point in the east, where it enters a proglacial lake at 1049 m a.s.l. The glacier has a surface area of about 0,38 km^2 (Andreassen, Winsvold, Paul, & Hausberg, 2012). The proglacial lake covers an area of ~5500m^2 (Kartverket, 2010).

The Skjerdingane glacier is situated below the glacial threshold for the inner parts of Sogn og Fjordane, which is estimated to be at about 1400 m a.s.l. The glacial threshold is calculated by taking the average height between the highest suitable peak without a glacier, and the lowest peak with a glacier. This is said to be the critical height at which a glacier can exist. (Nesje, 2012) This makes the Skjerdingane cirque glacier of particular interest for investigations on glaciers and glacier hydrology.

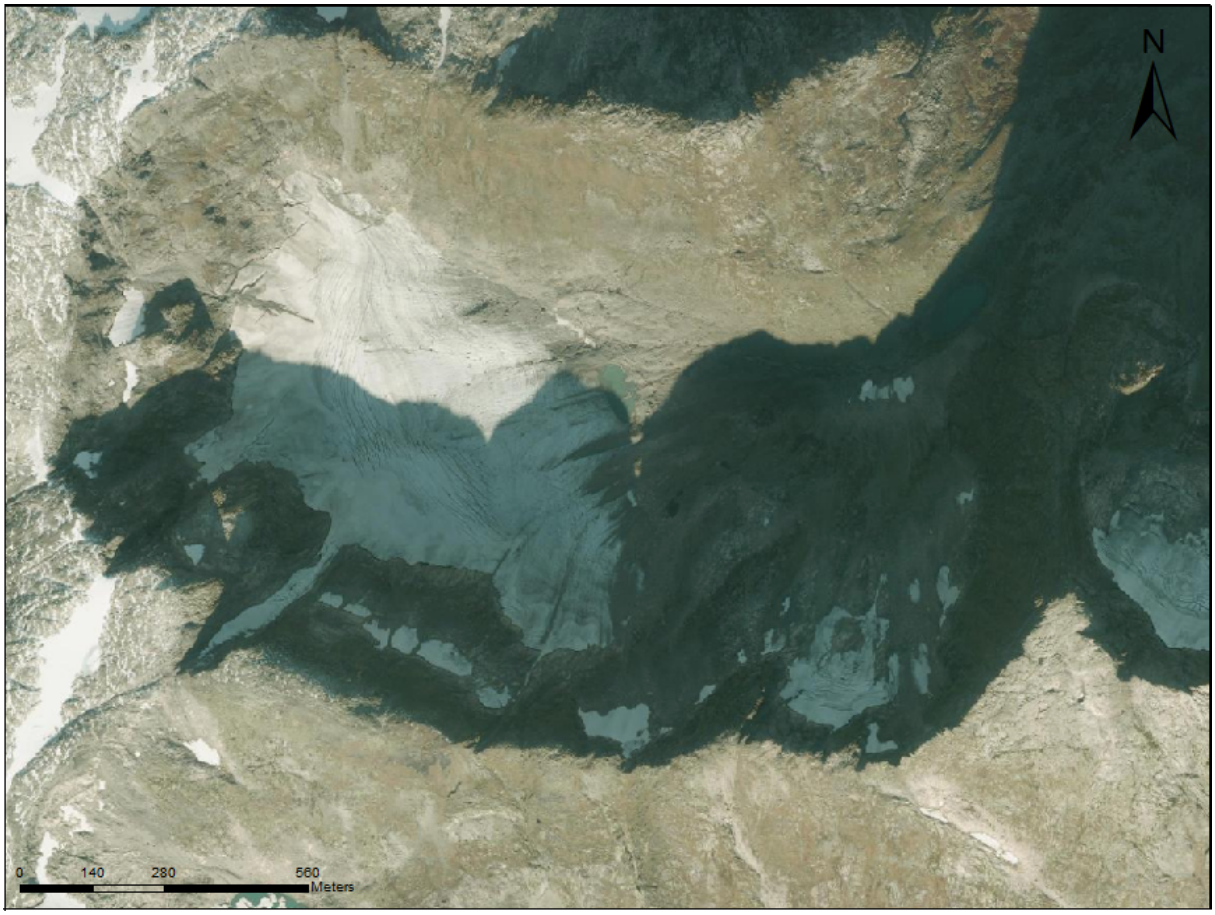

Figure 1.2 Areal image of Skjerdingane. The cirque glacier is seen to the left, with the proglacial lake directly in front of it. The proglacial stream is running between the glacial lake and the valley lake, which lies in the shade in the upper right quadrant of the picture. (Kartverket)

The glacial lake feeds a proglacial stream. The stream passes through another lake at 960 m a.s.l. before it flows down into Frudalen as Tungelvi, where it joins Frudalselvi. The valley lake has a surface area of ~7900m^2. The exact length and fall of the river between the two lakes has been measured with GPS to be 610 meters long, with a vertical drop of 89 meters.

2 Theoretical background

2.1 Numerical model

2.1.1 Modelling diffusion in one dimension

To better understand how Rhodamine WT acts as it is diffused in water, we developed a numerical model. The model assumes that the processes driving diffusion of dye in water are the same as for heat conduction: in the same manner as heat flows from areas with higher heat to areas with lower heat, a cloud of dye will diffuse from an area with high concentration, to an area with lower concentration.

To simplify this process, we have only looked at how diffusion works in one dimension. The model uses the 1D Heat Equation, which models how heat (u) spreads across a one dimensional bar with a length (x) ranging from 0 to L. (Piccolo, 2016) Further on we will refer to this equation as the diffusion equation, and use it to predict how a concentration of rhodamine WT will diffuse over space and time using finite difference modelling in excel.

2.1.2 Altering the diffusion equation

The diffusion equation is shown in equation (1)

$$(1)\ \frac{\partial u}{\partial t} = D\frac{\partial^2 u}{\partial x^2}, \qquad 0 < x < L \quad and \quad t > 0$$

with the boundaries:

$u(0, t) = U_0$ and $u(L, t) = U_L, \ \forall t > 0$

and initial conditions:

$u(x,0) = f(x), \qquad 0 < x < L$

where u is the concentration of dye, t is time, x is distance and D is the thermal diffusivity. D is given as $D = \frac{k}{c_p \rho}$, where k is thermal conductivity, c_p is specific heat capacity, and ρ is density. U_0 is the concentration at one end of the diffusion system, while U_L is the concentration at the other end.

To create a finite difference model, we need to approximate the partial derivatives with difference quotients, and set the relationships between u at (x, t), and its neighbouring values at a distance Δx apart and a time Δt later (Lau, 2016; Piccolo, 2016).

The difference quotient for an estimation forward in time (t+Δt) is taken from the partial derivative for time, as shown in equation (2). The letters in brackets show which factors the variables are dependent on.

$$(2)\ \frac{\partial u}{\partial t}(x,t) = \frac{u(x,t+\Delta t)-u(x,t)}{\Delta t}$$

The difference quotient for variation in space is derived by knowing the curvature of the u-value at the time t. The curvature of the line at point u (∂x^2) is given by the values of u(x-Δx), u, and u(x+Δx), shown in equation (3). If the curvature of the line is convex the value will be negative (the values of u(x-Δx) and u(x+Δx) is lower than the value of u), and if the curvature is concave the value will be positive (the values of u(x-Δx) and u(x+Δx) are higher than the value of u).

$$(3)\ \frac{\partial^2 u}{\partial x^2}(x,t) = \frac{u(x+\Delta x,t)-2u(x,t)+u(x-\Delta x,t)}{\Delta x^2}$$

By substituting equation (2) and (3) into equation (1) we get the equation (4):

$$(4)\ \frac{u(x,t+\Delta t)-u(x,t)}{\Delta t} = D\,\frac{u(x+\Delta x,t)-2u(x,t)+u(x-\Delta x,t)}{\Delta x^2}$$

By rearranging the terms in equation (4) for u(x, t+Δt) we get equation (5):

$$(5)\ u(x,t+\Delta t) = u(x,t) + K\{u(x+\Delta x,t) - 2u(x,t) + u(x-\Delta x,t)\}$$

Where

$$(6)\ K = D\left(\frac{\Delta t}{\Delta x^2}\right)$$

Equation (5) states that by knowing u at three adjacent points (x+Δx , x, and x-Δx) at the time t, we can calculate what value u has at position x, and at a time t+Δt (Piccolo, 2016), which can be used to simulate how an initial concentration of dye will spread out over time.

2.1.3 Introducing movement in the model

Next, we want to add movement to model how dye diffuses along a plug flow. A plug flow moves along with equal speed across the whole cross-sectional area of the flow, without friction along the sides or turbulence. The goal here is to move the diffusion process along x as t increases.

By finding Δu between each value of u and dividing by Δx, we divide Δx into smaller increments. By multiplying with Δx*v, where v is the velocity for the stream, we decide how many time steps it takes to move the distance Δx. The expression is shown in equation (7).

(7) $u_x^{t+1} = (u-1) + \frac{u-(u-1)}{\Delta x}\Delta x v$

2.1.4 Applications of the model

The numerical model can be adjusted manually as an aid to understanding the effects of the different parameters; Δt, Δx, v and D. By mimicking the breakthrough curve of an actual measurement over the same time, distance and concentration value. According to Seaberg et al. (1988) the diffusion coefficient (D) in the numerical model, should correlate to the dispersion coefficient in streams.

When using differential equations or other algorithms for modelling, it is important to consider convergence. Our model starts to misbehave by rapid fluctuation when the value of K > 0,42. For the model to work we must choose Δx and Δt small enough to get a suitable resolution, but still making sure of having the relationship $K=D(\Delta t/\Delta x^2)$ less than 0,42. (Lau, 2016)

2.2 Dye tracing theory

2.2.1 Fluorescent dyes

Fluorescent dye tracing relies on the naturally occurring phenomenon *fluorescence*. Fluorescence is a physical reaction in which an atom absorbs light of a given wavelength, and immediately emits light of a different wavelength. As detailed in "Fluorometric procedures for dye tracing" by Wilson et al. (1968), the fluorescing atom first absorbs light of a given wavelength (i.e. from sunlight, or in dye tracing; from a UV light), which delivers energy to the atom. The energy goes towards bumping an electron into a higher energy orbit; the "excited state" of the atom. The excited state is unstable, and the electron promptly returns to its original orbit, the "ground state" of the atom. It is at this step light is emitted. Due to an effect called Stokes' shift, some energy is lost in the exchange, and the result is that the emitted photon generally has a longer wavelength and lower frequency than that of the absorbed photon. (Wilson et al., 1968)

Because the light absorbed and emitted by the fluorescing substance is of different spectra, the effect is well suited for accurately measuring concentration in a solution (Smart & Laidlaw, 1977). The light source used to elicit the fluorescence can be tailored to only emit light in the absorption spectrum of the fluorescent substance, while the receiving sensor can be tailored to only register light from the emission spectrum of the substance. This allows for very precise measurements of very low concentrations (down to 0,01 ppb in the case of Rho-

damine WT) (Smart & Laidlaw, 1977). While many materials are fluorescent to some degree, the dyes used in fluorometry are especially good at returning a large amount of the absorbed light, as emitted light (Wilson et al., 1968). In this project, we have used the fluorescent dye Rhodamine WT, which has a specific gravity of 1.15g per ml (Turner Designs). Rhodamine WT is related to Rhodamine B, commonly used in the 60s (Turner Designs).

2.2.2 Parameters which affect the fluorescence of dyes

Several variables influence the behaviour and measurements of dyes during water tracing. The temperature and pH of the water directly influences the fluorescence of the dye, while photochemical decay, quenching and sorption effects may effectively remove dye from the sample (Smart & Laidlaw, 1977). Below is a more detailed overview of these effects.

Temperature has a large impact on the fluorescence of a solution with fluorescing dye in it, second in importance only to the actual concentration (Wilson et al., 1968). The intensity of fluorescence varies inversely with water temperature, with the rate determined empirically for every type of dye (Smart & Laidlaw, 1977). The fluorescence of Rhodamine WT varies inversely with temperature according to equation 8:

(8) $$D_{T0} = D_T e^{0.027(T-T0)}$$

where D_{T0} is fluorescence at the device calibration temperature T0, and D_T is the fluorescence at temperature T (Clark, Lenain, Feddersen, Boss, & Guza, 2014).

Fluorescence of a sample may also be affected by pH values, but this is generally not an issue outside of highly acidic streams. The effect of pH on fluorescence varies between dyes. For Rhodamine WT, the stable region is between pH 5-10, with lower or higher pH resulting in a decrease in fluorescence. (Wilson et al., 1968)

Photochemical decay occurs when fluorescent dyes are exposed to sunlight, and results in a permanent reduction in fluorescence (Wilson et al., 1968). All dyes will be affected to some degree, especially if exposed over long distances or long time periods during sunny days (Wilson et al., 1968). Rhodamine WT has been shown to be more resistant to photochemical decay than other dyes used in dye tracing (Smart & Laidlaw, 1977).

Quenching is an effect which results either from other chemicals in the sample, or from a relatively high concentration of dye in the sample. In the first case the effect can arise from several different causes, depending on the kind of chemicals present in the sample to be measured.

Common chemicals, such as chlorine in chlorinated tap water, can absorb some of the light the apparatus sends out to excite the dye, or absorb some of the light from the excited dye before it reaches the sensor, thus reducing the detected signal. Chemicals can also reduce the excited-state energy of the fluorescence reaction, or chemically react with the dye and change its properties in other ways. In the second case, very high concentrations (above ~40 million ppb for Rhodamine WT) of dye in a sample might lead to concentration quenching, where the dye in itself blocks the passage of light absorbed by and emitted by the dye before it reaches the fluorometer. (Wilson et al., 1968)

Sorption of dyes includes two different processes. *Adsorption* occurs when dye adheres to objects in the water, either static objects like aquatic plants and the material in the riverbed, or moving objects like suspended particles. Some researchers have reported recovery of Rhodamine WT as low as 45% due to sorption effects in mountain streams (Bencala et al., 1983). Others have not found such a severe effect (Smart & Laidlaw, 1977). *Absorption* on the other hand, occurs when objects in the water absorb the dye, and does not have a large effect on fluorescence of dyes in mountain streams (Wilson et al., 1968).

2.2.3 Slug injection and discharge measurements

Slug injection is a dye tracing method which is used to measure the discharge of streams. It relies on injecting a single highly concentrated dose of dye at one point in the stream, and measuring the dispersion of that dye at a point downstream (Kilpatrick & Cobb, 1985). When fluorescence is measured at a point in the stream and plotted against time, it produces a time-concentration curve called a *breakthrough curve*. The area under the breakthrough curve is used to calculate the dispersion of the dye. Measurements of discharge with the slug injection method uses the relation in equation 9:

$$Q = \frac{M}{A_c} \tag{9}$$

where Q is the volume rate of flow of the stream, M is the mass of injected dye and A_c is the area under the breakthrough curve, which represents the dispersion of the dye (Kilpatrick & Cobb, 1985). The validity of this equation relies on several assumptions. Most importantly, the breakthrough curve must be measured far enough downstream to allow for sufficient lateral mixing. The equation assumes full recovery of the injected dye, which makes it important to continue the measurement to include the drawn-out tail of the breakthrough curve. Lateral mixing relies on the attributes of the stream to be measured. Stream depth is

essential for good mixing. Shallow, white water streams and braided streams can give the illusion of good mixing, but in reality, have poor lateral mixing conditions. (Kilpatrick & Cobb, 1985)

2.2.4 Breakthrough curve analysis

Breakthrough curves can be analysed to calculate several parameters of the sampled water flow (Fyffe, 2013). After finding the peak concentration, the time from injection to peak (t_m) can be used to calculate the average trace velocity:

$$u = \frac{d}{t_m} \quad (10)$$

Where u is the trace velocity of the stream (m s^{-1}), and d is the distance from dye injection to measuring point in a straight line (m) (Fyffe, 2013; Seaberg et al., 1988) Since a straight line from injection point to measuring point is used and the water necessarily takes a longer path, the trace velocity u will represent a minimum velocity for the water (Fyffe, 2013).

After integrating the area under the breakthrough curve, equation 9 can be arranged to calculate the discharge of the stream:

$$Q = \frac{S_g V_i C_i}{A_c} \quad (11)$$

Where Q is the average flow of the stream (m^3 s^{-1}), S_g is the specific gravity of the dye, V_i is the volume of dye added (m^3) and C_i is the concentration of that dye (ppb). A_c is the area under the breakthrough curve (ppb s). As stated above, a precise estimate for Q relies on good lateral mixing and full recovery of the breakthrough curve. (Kilpatrick & Cobb, 1985)

By dividing the flow of the stream by its trace velocity, an estimation of the cross-sectional area of the stream can be found:

$$A_{sm} = \frac{Q}{u} \quad (12)$$

Where A_{sm} is the apparent mean cross sectional area (m^2), Q is the average flow of the stream (m^3 s^{-1}) and u is the trace velocity of the stream (m s^{-1}) (Fyffe, 2013; Nienow, Sharp, & Willis, 1998)

2.2.5 Dye dispersion

As a cloud of dye travels down the stream, it is subject to both lateral and longitudinal mixing. This mixing process is called dispersion. The dispersion is primarily due to turbulent flows, velocity variation, and convection in the stream. The process of diffusion takes place simultaneously, but compared to the above mentioned factors it does not have a substantial effect on the total dispersion of the dye cloud (Seaberg et al., 1988). Turbulence is dependent on the streams Reynolds number (Re) in equation 13. Where a low value Re < 1000 suggests a laminar flow, and a high value of Re > 2000 suggests the stream to be turbulent. (Falkovich, 2011)

$$(13) \quad Re = \frac{QR_H}{vA}$$

Where Q is the streams discharge, v is the fluids kinematic viscosity, A is the streams cross sectional area, and RH is the hydraulic radius given by A divided by the streams wetted perimeter (Chapman, 2002).

The dispersion coefficient (D[m^2 s^{-1}]) gives us the rate at which a dye cloud spreads relative to the rate of the stream (Willis et al., 1990). It can be estimated from the breakthrough curve using equation 14.

$$(14) \quad D = \frac{d^2(t_m - t_i)^2}{4t_m^2 t_i ln\left[2\left(\frac{t_m}{t_i}\right)^{\frac{1}{2}}\right]}$$

Where d is the straight-line distance from the injection point to the measuring point, t_m is time from injection of dye to the peak concentration, t_i (where I = 1 or 2) is time from the injection time to half of the peak concentration value. (t_1 on the leading edge and t_2 for the falling limb). The equation is solved, according to Fyffe (2013), iteratively for both variations of t_i, subtracting equation (13) for t_1 from equation (13) for t_2, and varying t_m until the variation between the two equations approaches zero. The final value of t_m is then used to solve the equation again to obtain a value for D.

The dispersion is proportional to the streams velocity (u[m s^{-1}]). By using equation 15 we find the ratio of the proportionality, called the dispersivity (α [m]). (Seaberg et al., 1988)

$$(15) \quad D = \alpha u \quad \rightarrow \quad \alpha = \frac{D}{u}$$

In glacier hydrology investigations, more dispersed breakthrough curves with $\alpha > \sim 10$ indicates underdeveloped subglacial drainage systems, while less dispersed breakthrough curves with $\alpha < \sim 10$ are typically of efficient and well developed systems. (Hubbard & Glasser, 2005)

3 Methods and experimental setup

3.1 Numerical modelling

3.1.1 Setting up the numerical model in excel

The first step in setting up the numerical model in excel, is to set the time (t) and space (x) intervals. For the first model, the x-interval ranging from [0,1] is set to a distance of Δx = 0,05, the time interval Δt is set to 0,004, and D to 0,2.

The initial set up of the numerical model in excel is shown in figure 3.1. The constants are defined at the top of the excel sheet, where Δx sets the spatial interval on the x-axis, Δt sets the time interval along the y-axis. In row 7, the light green row along the x-axis, is where the initial conditions are set. In figure 3.1 the initial conditions are all 0 except for cell N7, which is 1. The light green column (excel column "D" in figure 3.1) are Dirichlet boundaries. The differential equation has two boundaries, one at each end. The model aims to reach equilibrium with its boundary values, as time passes by.

	A	B	C	D	E	F	G	H	I	J	K	L	M	N
1														
2		Δx=	0,05 m		Δt=	0,0040 sec		D=	0,2	K=	0,32			
3														
4														
5			x	0	0,05	0,1	0,15	0,2	0,25	0,3	0,35	0,4	0,45	0,5
6		t												
7		0		0	0	0	0	0	0	0	0	0	0	1
8		0,004		0	0	0	0	0	0	0	0	0	0,32	0,36
9		0,008		0	0	0	0	0	0	0	0	0,1024	0,2304	0,3344
10		0,012		0	0	0	0	0	0	0	0,032768	0,110592	0,22272	0,26784
11		0,016		0	0	0	0	0	0	0,01048576	0,04718592	0,12156928	0,20127744	0,2389632
12		0,02		0	0	0	0	0	0,00335544	0,01887437	0,05924454	0,12327322	0,18783027	0,21484431
13		0,024		0	0	0	0	0,00107374	0,00724776	0,02682677	0,06681526	0,1234423	0,17581651	0,19755533
14		0,028		0	0	0	0,0003436	0,00270583	0,01153736	0,0333578	0,0721396	0,12208139	0,16601318	0,18364248
15		0,032		0	0	0,00010995	0,00098956	0,004776	0,01569381	0,03878543	0,0757108	0,12015819	0,15759639	0,17235973
16		0,036		0	3,5184E-05	0,00035624	0,00191975	0,00705804	0,01958943	0,04321223	0,07811785	0,11791525	0,15034043	0,16291119
17		0,04		0	0,00012666	0,00075383	0,00306368	0,00942383	0,02313868	0,04682273	0,07968322	0,11555614	0,14398702	0,15486591
18		0,044		0	0,00028682	0,00129229	0,00435977	0,01177734	0,02632883	0,04975919	0,0806472	0,11317469	0,13837038	0,14790342

Figure 3.1 Shows how we set up the numerical model in excel. Distance(x) is shown in dark green, time(t) in blue, diffusion coefficient(D) in orange, K-value in yellow. Boundary conditions are set up in the columns at x=0 and x=1, and the initial values are at t=0. The image is cropped; the x-axis goes all the way to 1.

The model itself is created by applying equation 16 inside each cell in the frame, made by the boundary conditions and initial values. Equation 16 is the same as equation (5), without the variable notation.

$$(16) \quad u_n^{k+1} = u_n^k + K(u_{n+1}^k - 2u_n^k + u_{n-1}^k)$$

Where u_n^{k+1}, the concentration of u at x_n in space and t_{k+1} in time, is affected by the concentrations at the three neighbouring points u_{n+1}, u_n, u_{n-1}, at their previous time step t_k.

3.1.2 Defining Dirichlet boundary conditions

Dirichlet boundary conditions are stationary boundaries with a set value for u at both ends of the model (Lau, 2016). Figure 3.2 shows the diffusion process for all values of x, at different times. When the Dirichlet boundary conditions are set to 0 the model will continuously let dye out, the concentration throughout the model is 0.

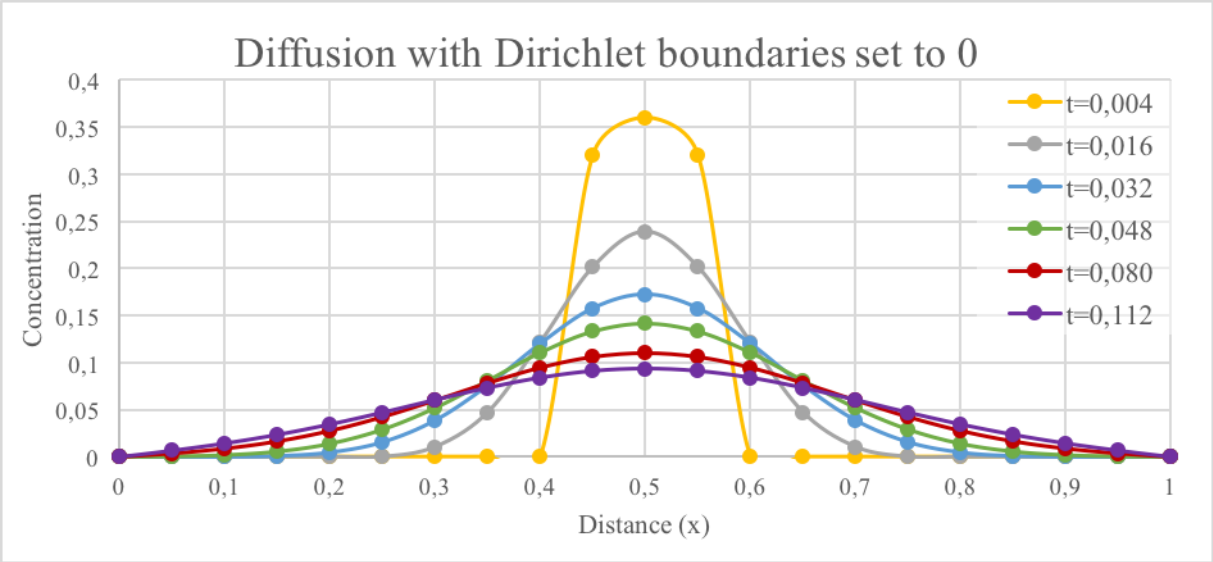

Figure 3.2 This plot shows the dye concentration at different locations. The plotted lines each correspond to a time step, with the sharpest peak being the concentration at t=0,004, and so on. Because the Dirichlet boundary condition are set to 0, dye "leaks out" of the system, and eventually the concentration will be 0 along the entire x-axis.

The derivative boundary conditions are set up by creating a new column outside the boundary columns, which mimics the value on the opposite side of the boundary. In figure 3.3 column D copies F and column Z copies X. Then applying equation 16 in the boundaries themselves (Column E and Y).(Piccolo, 2016)

	A	B	C	D	E	F	G	H	I	J	K	L	M	N	O
1															
2			Δx=	0,050	m.	Δt=	0,0040	sec.	D=	0,2	K=	0,32			
3															
4				-0,550	-0,500	-0,450	-0,400	-0,350	-0,300	-0,250	-0,200	-0,150	-0,100	-0,050	0
5				x	0	0,05	0,1	0,15	0,2	0,25	0,3	0,35	0,4	0,45	0,5
6	t														
7	0			0	0	0	0	0	0	0	0	0	0	0	5073,5295
8	0,004			0	0	0	0	0	0	0	0	0	0	1623,5294	1826,4706
9	0,008			0	0	0	0	0	0	0	0	0	519,52942	1168,9412	1696,5883
10	0,012			0	0	0	0	0	0	0	0	166,24941	561,09177	1129,9765	1358,8941
11	0,016			0	0	0	0	0	0	0	53,199813	239,39916	616,78533	1021,187	1212,3868
12	0,02			0	0	0	0	0	0	17,02394	95,759663	300,57894	625,4303	952,96243	1090,019
13	0,024			0	0	0	0	0	5,4476608	36,771711	136,1064	338,98921	626,28814	892,01024	1002,3028
14	0,028			0	0	0	0	1,7432515	13,728105	58,535116	169,2418	366,00237	619,38355	842,27278	931,71555
15	0,032			0	0	0	0,557840468	5,0205642	24,231195	79,623011	196,77904	384,12097	609,62613	799,56992	874,47218
16	0,036			0,1785089	0	0,1785089	1,807403116	9,7398946	35,809174	99,38756	219,23853	396,3332	598,24649	762,75663	826,53473
17	0,04			0,6426322	0,1142457	0,6426322	3,824554248	15,543667	47,812088	117,39479	237,55651	404,27516	586,27748	730,52238	785,71674
18	0,044			1,4917636	0,4524131	1,4917636	6,556455215	22,119446	59,752657	133,58008	252,45473	409,16593	574,1951	702,02621	750,39235
19	0,048			2,7798727	1,1175974	2,7798727	9,91591082	29,181916	71,334803	147,99519	264,56243	411,82768	562,29172	676,59742	719,43802
20	0,052			4,5314768	2,1814536	4,5314768	13,79750036	36,505718	82,377203	160,76538	274,38579	412,85129	550,72105	653,72859	692,02003
21	0,056			6,7445969	3,6854685	6,7445969	18,09900257	43,917964	92,782545	172,0397	282,33622	412,66066	539,56514	633,01944	667,51351

Figure 3.3 Derivative boundary conditions applied to the numerical model, set up in excel. The derivative boundary conditions can be seen in excel column D. This column mimics the F column, which is inside the system. This is done to contain the dye inside the system, without any dye leaking out at the boundaries.

The boundary conditions will adapt according to the concentration inside the boundary. The model will not lose any dye, and will over time even out at some concentration > 0. An example of this is shown in figure 3.4.

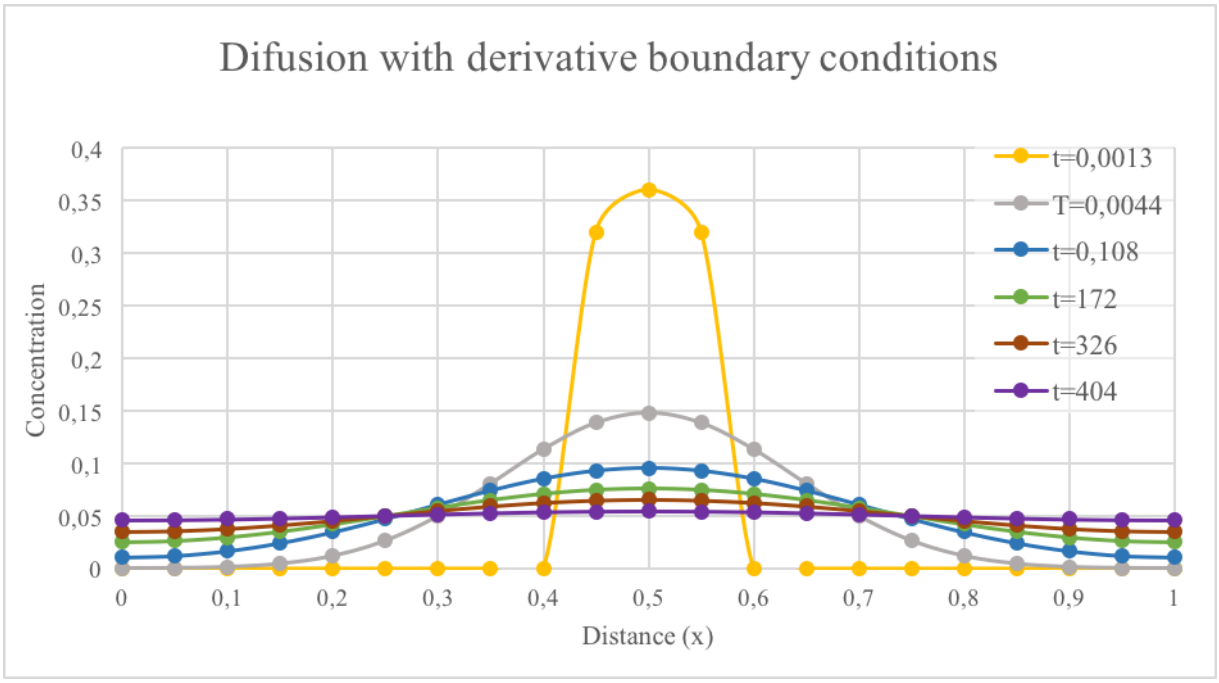

Figure 3.4 This plot again shows the dye concentration at different locations, this time with derivative boundary conditions. Because no dye leaves the system, the final equilibrium concentration will be above zero.

3.1.3 Modelling diffusion in still standing water

We simulated two models of diffusion in still standing water. In the first simulation, the numerical model simulated concentrations of ppb when a drop of rhodamine was injected in the centre of the system and is measured at the far end of the system. (in figure 3.4, the

injection point would be x=0,5 and the measuring point at x=1). Δx was set to 0,077m, the whole length of the system is 1,54cm. Δt=300 seconds, K= 0,3035 and the diffusion coefficient D is $6*10^{-6}$. In the centre of the model it is injected 10147 ppb, representing 10µl of Rhodamine WT diluted in one cell of 0,0976 litres of water.

The second simulation should simulate the same closed system, with the fluorometer placed 15 cm from the injection point. Δx was set to 0,077m, and the whole length of the system is 154cm. Δt=800 seconds, K= 0,202 and the diffusion coefficient D is $1,5*10^{-6}$. In the centre of the model it is injected 5073 ppb, representing 5µl of Rhodamine WT diluted in one cell of 0,0976 litres of water.

3.1.4 Modelling dispersion in moving water

To introduce movement of the water in the simulated system, equation (7) is implemented into equation (5), so that the diffusion process and movement occurs simultaneously. The diffusion equation with movement is presented in equation 17, the movement expression is emphasized with square brackets. The result on the simulation is shown in figure 3.5.

$$(17) \qquad u_n^{k+1} = u_n^k + K\left(u_{n+1}^k - 2u_n^k + u_{n-1}^k\right) + \left[u_{n-1}^{k+1} + \frac{u_n^{k+1} - (u_{n-1}^{k+1})}{\Delta x} \Delta x v\right]$$

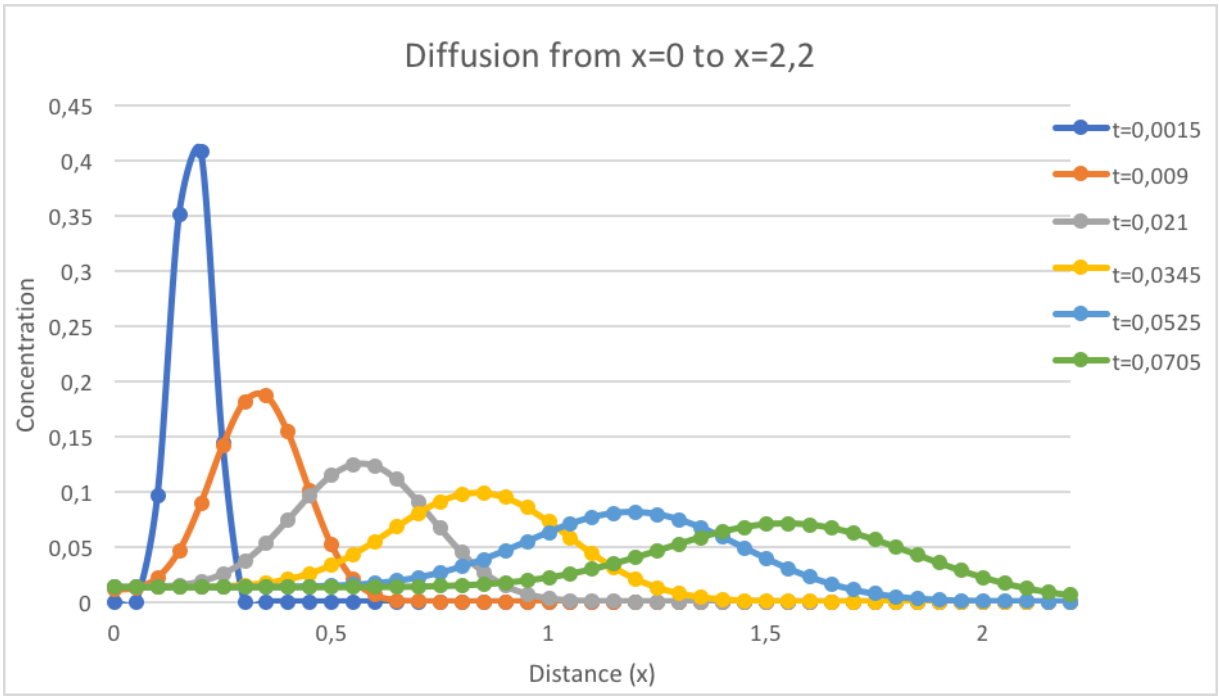

Figure 3.5 This plot shows the dye concentration at different locations, with movement added to the model. The curves each represent a different time-step. The initial concentration is an isolated peak concentration, seen to the left. It spreads out over time like before, yet now it also moves along the x-axis towards the right.

The upstream boundary is derivative, to avoid dye being removed from the system by diffusion in the upstream direction. The injection point is set at a distance away from the upstream boundary, to avoid any disturbance from interactions with the derivative boundary condition. Neither the derivative- nor Dirichlet boundary conditions are ideal to use at the downstream end of the model.

To prevent influence from the boundaries, the x-axis is extended for much longer than the modelled gutter-length, and set a Dirichlet boundary to 0 at the end. From the point where the "dye" hits the boundary, is the time (t) where the model may be affected by the lack of optimal boundaries. The Dirichlet boundary will rapidly reduce the concentration to 0.

3.2 Dye tracing techniques

3.2.1 Rhodamine WT

For our project, we have used the commercially available dye "Keyacid Rhodamine WT Liquid". It is a solution with approximately 21% active dye ingredient and is specifically designed for water tracing. (Keyacid Rhodamine WT, 2002).

3.2.2 The fluorometer: Cyclops 7 and DataBank

The instruments used were the Turner Designs Cyclops 7 sensor and the Turner Designs DataBank Handheld data logger, (when combined simply referred to as the fluorometer). The Cyclops 7 is configured for dye tracing of Rhodamine WT, and the LED outputs light at 530nm. This gives an excitation of the Rhodamine WT at 535nm, and the sensor receives emitted light in the 590-715nm ranges. Compared with the optimum wavelength peaks stated by (Wilson et al., 1968), this is lower than 558 nm for excitation and higher than 582 nm for emission, to avoid overlapping of wavelengths. The Cyclops 7 can detect concentrations of Rhodamine WT down to 0.01 ppb, and has a linear range from 0-1000 ppb. At each measurement, the DataBank applies one of three gain settings (low, medium, high), based on the concentration at that time. (Turner Designs)

Figure 3.6 The fluorometer in use. Anders is holding the DataBank, while the Cyclops 7 is submerged in the proglacial stream. Photo: Jan Hedges

The DataBank is attached to the Cyclops 7 sensor during use, and can store up to 9999 measurements (Turner Designs). It has a minimum logging interval of 1 second, and for each logged value it takes the average of the last ¼ second, while updating 30 times a second (2017). The DataBank has a maximum of 16 channels, which can be device calibrated separately, however we only used two channels, and both were calibrated the same way.

Device calibration of the DataBank was performed in the simplest way; the Cyclops 7 is submerged in clean (ideally purified) water and recalibrates this as a reference blank value (no fluorescence should be present). Then it outputs all further readings as RFUB (Raw Fluorescent Units Blanked). This calibration was done with purified water for the field measurements, and with clean tap water for the lab experiments. RFUB is the DataBanks own dimensionless unit for displaying fluorescence in a linear fashion (the mV values themselves are not linear, as they return to and reuse low mV values for each gain setting). In our project, we will ignore the RFUB values, and only use our own separate calibrations to calculate Rhodamine WT concentrations from the raw mV values.

The DataBank stores date, time, gain setting, mV and RFUB. The stored values were imported from the DataBank using Turner Designs own DataBank GUI software, and further processing was done in Microsoft Excel.

3.2.3 Dye measuring and dye injection methods

To measure up quantities of Rhodamine WT we used pipettes. As the range of dye quantities used was wide, from up to a hundred millilitres used in the field to fractions of a microliter in the lab, we used a variety of different pipette sizes. These were tested with precise measuring scales; the internal variation was 2% for the small pipettes and 1% for the smaller pipettes. One systematically inaccurate pipette (size 40-250µl) was found to be measuring up a larger dose (11 µl) than stated. Whenever this was used, it has been accounted for in the calculations.

For the field experiments, quantities of dye in the 50ml-100ml ranges were pre-measured into sealed plastic bottles. When these were poured into running water, the bottles were flushed thoroughly to make sure all of the dye was used. For injections without access to running water (i.e. on the glacier), separate bottles of water were brought along for flushing out the remaining dye.

At the start of the laboratory experiments, two concentrations of diluted Rhodamine WT were measured up and stored in sealed plastic bottles out of direct light. These were 1/50000 and 1/100000 solutions of Rhodamine WT and tap water. We also used injections of pure Rhodamine WT for some experiments; these were measured and injected directly by pipette.

3.2.4 Calibration procedure

To map the mV-values to their corresponding Rhodamine concentrations, we performed several rounds of concentration calibration. All the calibrations are based on the calibration procedure outlined by Fyffe in “Tracer Investigations”(2013). As we performed multiple calibrations, we will first describe the general procedure, and then list the variables that were changed in each instance.

For the calibration procedure, we used two buckets filled with five litres of water each, as seen in figure 3.7. The Cyclops 7 was submerged in the centre of the measurement bucket (2), with the sensor 5 cm above the bottom of the bucket. The DataBank and Cyclops 7 was switched on and measurements were started early, to gather background readings before the calibration started. A known quantity of Rhodamine WT dye was then added with a pipette to

the first bucket (1), and mixed thoroughly. The pipette tip was changed, and the pipette itself was rinsed. Next, a known quantity of the solution in bucket (1) was added to bucket (2), and the time of injection (from the display on the fluorometer) was noted. The new solution in bucket (2) was then mixed thoroughly, without disturbing the Cyclops 7. The concentration was given a set amount of time to settle, before another known quantity of the solution from bucket (1) was added to bucket (2). This was ideally repeated for enough steps to have a data set covering all three gain settings.

3.2.5 Concentration calculations

The concentrations of dye were calculated in parts per billion (ppb) for Rhodamine WT diluted in water. A formula was set up for calculating the concentration of Rhodamine WT in two buckets containing 5 litres of water. The concentration in ppb for bucket (1), $C_{(1)}$, was calculated using equation 18:

$$(18) \quad C_{(1)} = \frac{S_{g(d)} V_{i(1)} C_{(d)}}{V_{w(1)}}$$

Where $S_{g(d)}$ is the specific gravity of the dye, $V_{i(1)}$ is the volume of dye added to bucket (1) (ml), $C_{(d)}$ is the concentration of the dye (ppb) and $V_{w(1)}$ is the volume of water in bucket (1) (ml).

Similarly, the concentration in ppb for bucket (2) $C_{(2)}$ was calculated using equation 19.

$$(19) \quad C_{(2)} = \frac{S_{g(1)} V_{i(2)} C_{(1)}}{V_{w(2)}}$$

Where $S_{g(1)}$ is the specific gravity of the contents of the first bucket, $V_{i(1)}$ is the volume of solution from bucket (1) added to bucket (2) (ml), $C_{(1)}$ is the concentration of the first bucket (ppb) and $V_{w(2)}$ is the volume of water in bucket (2) (ml). Alternatively, a combined equation can be used to directly find the concentration in the measurement bucket (2):

$$(21) \quad C_{(2)} = \frac{V_{i(1)} V_{i(2)} S_{g(d)} C_{(d)}}{V_w(1) V_w(2)}$$

3.2.6 Lab calibration

In the lab, we performed the calibration procedure on five occasions, for a total of nine calibrations. The variables that were purposefully changed were the quantity of dye added to the first bucket, the quantity of solution from bucket (1) added to bucket (2) and the time allowed for the concentration to settle. The variables that we attempted to keep constant were the initial water levels in the buckets, the initial water temperature, and the light exposure of the

Cyclops 7. The water used for in the calibrations was tap water from the same faucet that was used during the experiments. The water contains small amounts of chlorine, which is shown to have an effect on the fluorescence of dyes (Smart & Laidlaw, 1977). Since the same water is used during the calibrations as in the experiments, we have not taken any further steps to mitigate the effects of chlorine.

Figure 3.7 The image shows the set up for the calibration procedure (here performed in Skjerdingane). Bucket (1) is to the left and bucket (2) to the right. The DataBank is in the centre, and the Cyclops 7 is suspended in bucket (2). Photo: Jan Hedges

3.2.7 Field calibration

We performed separate calibrations in the field, with water from the stream, to ensure that water temperature and water contents such as suspended sediments and chemicals were as close as possible to the actual field measurements. We did calibrations in the field on two occasions, following the same general steps as outlined in section 3.2.4. Due to time constraints, we varied the concentration increments by increasing the quantity of solution from bucket (1) added to bucket (2) several times throughout the calibration process. At one point, we also added a second quantity of dye to the first bucket (1), before continuing the process. During the field calibration, we used the shade cap on the Cyclops 7, which was also used during all the field measurements.

3.2.8 Accounting for temperature changes

The water temperature at device calibration (which is the instruments own calibration, described in section 3.2.2) was T0 = 7°C. To estimate T during every stage of our calibrations, we performed a test where we filled one of the calibration buckets with five litres of water and left it to heat up in the same room temperature as where we performed the calibration. We measured the temperature every twenty minutes to approximate the rate of change in temperature during our calibrations. This observed rate of change was used with equation 8 in the processing of our calibration data to correct the mV values according to the estimated temperature in the calibration buckets.

3.2.9 Generating the mV to concentration equations

After the measured fluorescence values (in mV) have been temperature corrected, they are plotted against the known concentrations (in ppb) from the calibrations. We then fit a linear regression model to the calibration dataset, which gave us a set of equations for converting mV values into concentration of Rhodamine WT (ppb). One equation was generated for each gain setting, and an IF(x)THEN(y)-formula was set up in excel to apply the correct equation to the mV values based on their gain value.

3.3 Lab methods

3.3.1 Diffusion experiment setup

The aim of this experiment was to investigate to what extent the dispersion of rhodamine WT in a simple experimental system with no flow component, can be approximated by the numerical model. The set up consisted of a piece of guttering sealed at the ends and filled with water. The dimensions of the gutter are 154 cm length, 10 cm width and 5,5 cm deep, containing 5,0 litres of water. Using this setup, there was conducted two experiments; one with the fluorometer positioned at the far end of the gutter and injecting 10 µl of rhodamine WT in the centre of the gutter (77cm from the censor). For experiment number two, the fluorometer was placed 15 cm from the injection point, and injected 5ul of rhodamine WT in the centre of the gutter. Figure 3.8 shows the setup, 10 minutes after starting diffusion experiment #1.

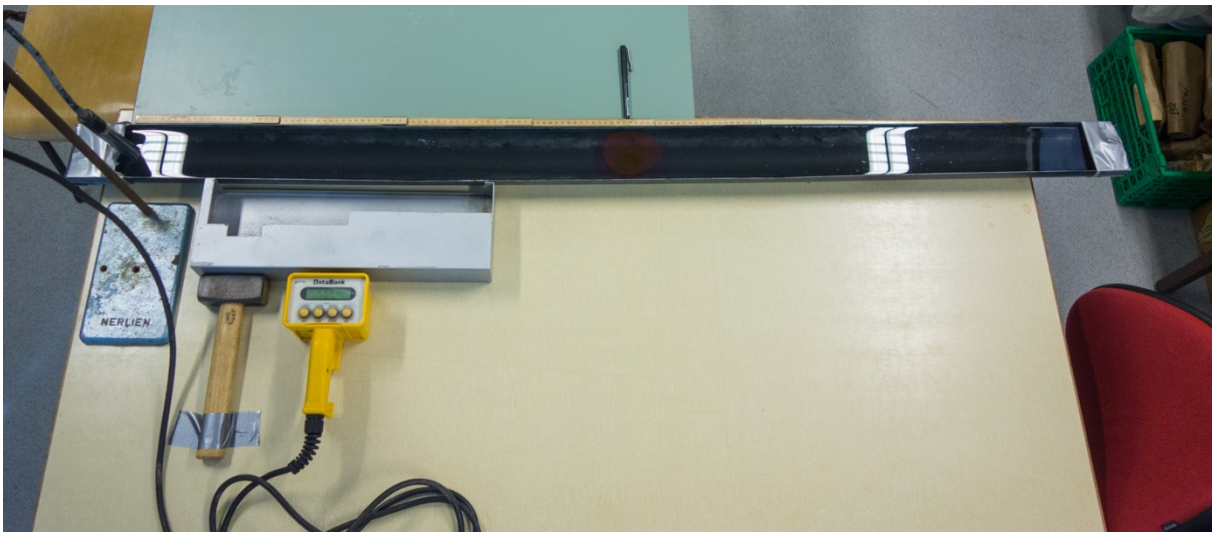

Figure 3.8 The setup for diffusion experiment #1, with stagnant water in the gutter and the Cyclops 7 placed at the far end. The image is taken five minutes after injecting 10µl Rhodamine WT in the center of the gutter. Photo: Jan Hedges

3.3.2 Siphon experiment setup

The siphon experiment consisted of three volumes of water connected by siphoning tubes. As seen in figure 3.9 and figure 3.10, two buckets and a large tub were used as water volumes, with two tubes connecting them. Water was supplied from a faucet, which was flowing at a constant rate into the top bucket (1). The top bucket (1) was kept continuously overflowing, to guarantee constant water pressure into the siphoning tubes. A plastic tube (2) then siphoned water from the top bucket and into the large tub (3). A second tube (4) siphoned water from the large tub and into the bottom bucket (5), which contained the Cyclops 7 sensor.

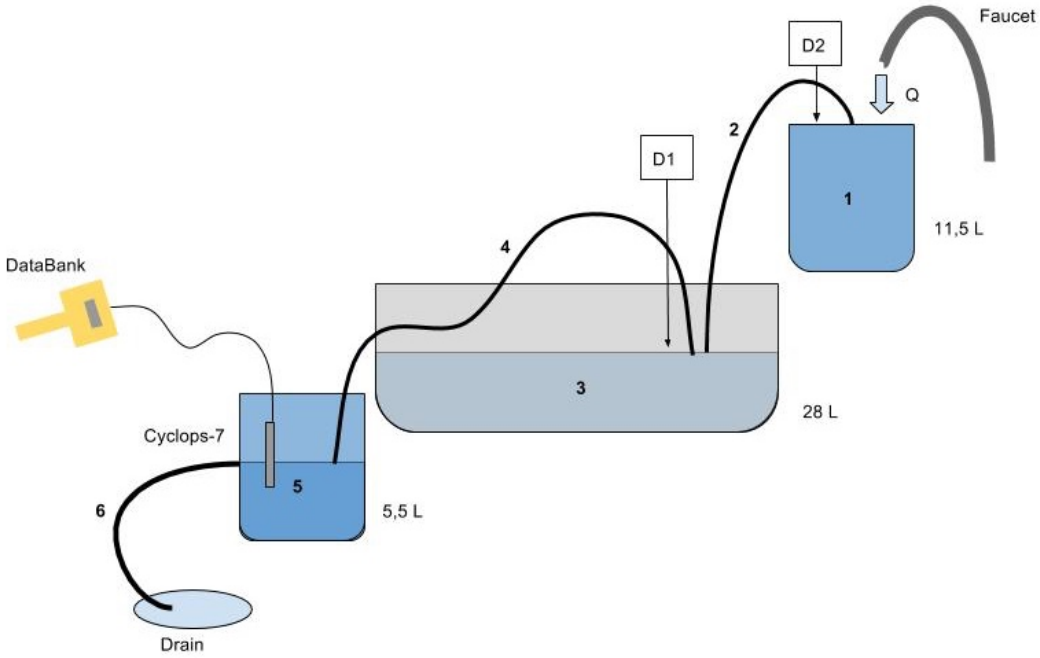

Figure 3.9 This sketch shows the setup for the siphon experiment. The setup includes two buckets (1 and 5), a tub (3), three siphons (2, 4 and 6), the DataBank and the Cyclops 7. The injection points are marked D1 and D2.

The diameters of the siphoning tubes were 6 mm. The first tube (2) was 144 cm long, while the second tube (4) was 149 cm long. The inflowing (2) and outflowing (4) tubes in the large tub were arranged so that they faced away from each other; which generated a slight circulation in the large tub. The bottom bucket (5) had an outflow pipe (6) plugged into it at the 5,5L mark, which emptied into an outlet drain. The plug connecting the outflow pipe to the bottom bucket had a diameter of 6mm, while the outflow pipe itself had a diameter of 13mm and a length of 124 cm.

Figure 3.10 This image shows the actual setup of the Siphon experiment. The pink bucket (1), the white tub (3) and blue bucket (5), with siphons connecting them.

The water level in the overflowing top bucket (1) was constant at 11,5 litres. The water level in the large tub (3) was constant at 28 litres, and the water level in the bottom bucket (5) was constant at 5,5 litres. We measured the flow at the lower siphon tube (4) by filling a container of known volume, while timing this with a stopwatch. The flow through the whole system was kept constant at Q=1L/60sec during all the measurements. The water temperature in the large tub was approximately 8℃ throughout the measurements.

The Cyclops 7 was placed in the centre of the bottom bucket for the whole duration of the measurements. A rigid stand was used to suspend the Cyclops 7 in the bucket 5,3 cm above the bottom. Two measurements were done, where dye was injected directly into the large tub (3), at two different quantities (5ml and 1ml 1/50000 Rhodamine WT/tap water mix). The injections were made at D1 where the first tube (2) delivered water into the large tub (3). Subsequently two measurements were done with the same amounts of dye, which were injected into the top bucket (1). The injections were made at D2, where the water from the faucet was entering the bucket. During the measurements using D2, the faucet was reduced to a low enough flow to avoid the top bucket from overflowing (as this would have allowed dye to leak out of the system). Instead the water level in the bucket was surveyed continuously, and the faucet flow was manually adjusted to maintain a stable water pressure, without the bucket overflowing.

3.3.1 Stream and basin experiment setup

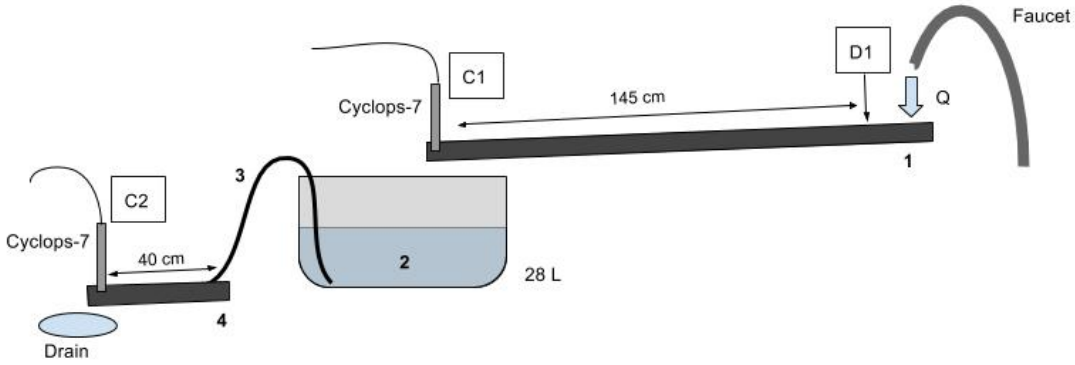

Figure 3.11 This sketch shows the setup of the stream and basin experiment. The setup consists an initial length of gutter (1), a basin (2), and a siphon (3) which moves water from the basin to the final length of gutter (4). D1 is the point of injection, while C1 and C2 are the measuring points.

The stream and basin experiment consisted of an open water flow system, with the option of passing the water through a basin and into another stream. As seen in figure 3.11 and figure 3.12, this was set up by using plastic gutter half pipe for the upper stream part of the system (1), and a sink for the basin part of the system (2). A plastic tube (3) was used to siphon water from the basin to the second piece of gutter half pipe in the lower stream (4). The diameter of the siphoning tube (3) was 12 mm, and the length was 97 cm. The water flow originated from a faucet at the start of the system, and the flow out of the system went into a drain. The rate of flow was measured at the faucet, by filling a container of known volume while timing this with a stopwatch.

In the first measurement, the top stream (1) was clean and empty. For all subsequent measurements, sediments were added to the gutter half pipe. The sediments were selected to match the diverse grain sizes in a mountain stream, and ranged from fine sand to coarse pebbles. The slope of the gutter half pipe was 1°. Water temperature was constant throughout the experiment at T = 8℃.

Figure 3.12 An image showing the stream and basin experiment, as seen from above measuring point C2. The initial gutter (1) is seen at the back of the image, the basin (2) and siphon (3) in the middle, and the final length of gutter (4) in the front. Photo: Jan Hedges

Initially the Cyclops 7 (C1) was first set up 145cm from the injection point (D1), submerged in the flow 3,2 cm above the bottom of the gutter. Data was gathered for this initial stretch at 1 measurement per second, with two different quantities of dye added at the injection point (P) (1ml and 250ml 1/50000 Rhodamine WT/tap water mix). This was done twice, at two different flow rates (Q=10L/1min16sec and Q=5L/1min 06sec), for a total of four measurements. Subsequently, the Cyclops 7 was moved to the gutter below the basin (4), 40 cm away from the outlet of the siphoning tube. The Cyclops 7 was submerged in the flow 3,2 cm above the bottom of the gutter. Data was then gathered at 1 measurement per second, with varying quantities of dye added at the injection point (P) (1ml, 250µl, 100µl, 50µl, 25µl and 10µl 1/50000 diluted Rhodamine WT). Water flow was kept constant at Q=2L/33sec. The water contained in the basin was constant at 28 litres for all measurements.

3.4 Fieldwork

3.4.1 Overview

The field measurements were carried out between the 28th of August and the 16th of October in 2016. In total, there were carried out seven field measurements and three field calibrations. The measurements are listed in table 1. Temperature data from the weather stations Frudalen and Anestølen(NVE, 2016b), as well as precipitation data for the area from Anestølen and Frudalen (NVE, 2016a).

Table 1. List of measurements and calibrations carried out in the Field. The IP and MP values refer to the field map (figure 3.13).

Measurement	Date	Weather	Description
#1.1	31.08.2016	100% cloud cover, some rain.	Field calibration
#1.2	31.08.2016	100% cloud cover, some rain.	Stream #1 (IP1-MP1)
#2.1	05.09.2016	Sunny, 5% cloud cover	Field calibration
#2.2	05.09.2016	Sunny, 5% cloud cover	Stream #2 (IP1-MP1)
#2.3	05-09.09.2016	Sunny, 5% cloud cover	Glacier #2 (IP2-MP2)
#3	11-15.09.2016	Partially cloudy (50%)	Glacier #3 (IP2-MP3)
#4	21-23.09.2016	Cloudy (70%), some rain the 22nd	Lake #4 (IP1-MP4)
#5	23-26.09.2016	Cloudy (90%), some rain the 24th	Supra-lake #5 (IP3-MP3)
#6	27.09-04.10.2016	100% cloud cover, pouring rain 27th-29th	Supra-stream #6 (IP3-MP2)

3.4.2 Field map

The field map in figure 3.13 shows where dye injections were done, labelled as injection points (IP) and where the fluorometer was set up, labelled as measuring points (MP).

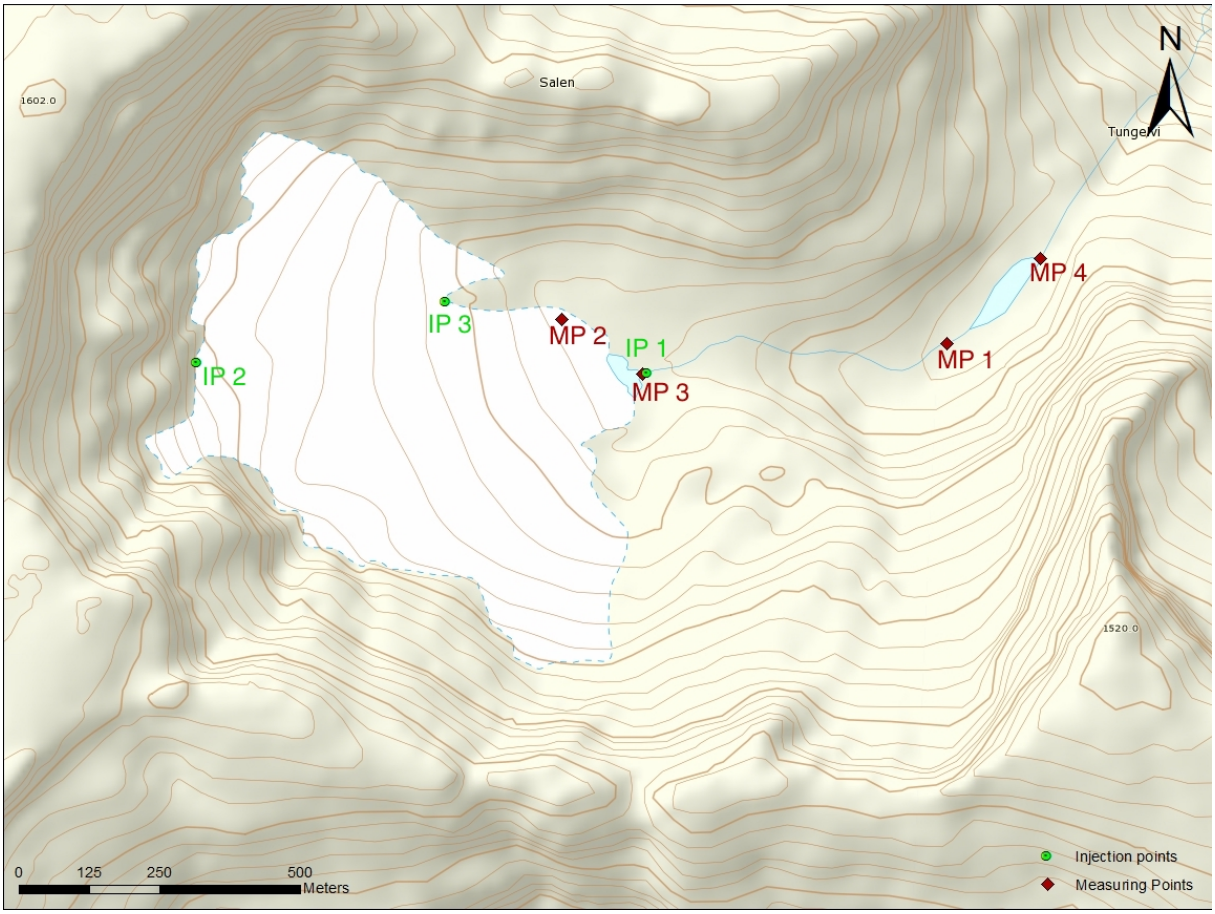

Figure 3.13 Field map showing the Skjerdingane cirque glacier, the proglacial lake, and the lake further down the valley.(Kartverket). Red points (MP) mark locations where we set up the fluorometer, and green points (IP) show locations where we injected the dye.

3.4.3 Using the fluorometer in the field

The set up used to position the Cyclops 7 in the stream is shown in figure 3.14. A length of accessory cord was attached to boulders on either side of the stream, and pulled tight about a metre above the water surface. A loop of another piece of cord was attached to a knot on the fixed line directly above the centre of the stream. This way we could slide the Cyclops 7 in and out of the stream, and adjust the tightness of the rope to vary the depth. The cable was run back to the DataBank along the fixed line and the DataBank was protected from moisture with a plastic bag.

Figure 3.14 This image shows how the Cyclops 7 was positioned in the stream, through use of a rope system attached on either side of the stream. Photo: Jan Hedges

The measurement points were chosen such that the Cyclops 7 could be positioned at a sufficient depth to avoid excessive exposure to sunlight. In addition to this we used the shade cap on the Cyclops 7 for all the field measurements.

3.4.4 Glacier measurements set up

We carried out two field measurements on the subglacial drainage system of the Skjerdingane cirque glacier. The first one, Glacier #2, was carried out on September 05th 2016. Injection of the Rhodamine WT was done at the back of the glacier (IP2), where a stream entered the chasm between the mountainside and the glacier, seen in figure 3.15. There is not an obvious outlet river from the Skjerdingane cirque glacier, but there is a proglacial lake. In the south part of the cirque, the glacier is lying into the glacial lake. In the north, a stream of water is exiting the glacier before it passes through an area dominated by moraine deposits and enters the glacial lake (the stream can be seen in figure 3.17 and 5.3). The fluorometer was set up in this stream, at MP2. Logging was started 15.30. 50ml of Rhodamine WT was injected at IP2 at 16.07. The measurement lasted until 21.30, when the DataBank ran out of free storage at 9999 recorded values.

Figure 3.15 Anders is pouring Rhodamine WT into the stream behind the glacier, at IP2. Note the cord attaching him to the crucial ice axe placement; safety first! Photo: Jan Hedges

The second glacier measurement, Glacier #3, was performed on September 11th 2016 with the same injection point (IP2), but with the fluorometer set up at the outlet of the glacial lake (MP3). Background logging was started at 16.10, 50ml of Rhodamine WT was injected at IP2 at 16.46. The fluorometer logged until 03.26 on the 15th of September.

3.4.5 Stream and valley lake measurements set up

Two field measurements, Stream #1 and Stream #2, were carried out in the proglacial stream originating at the glacial lake below the glacier. These were done during the course of a few hours on the 31st of August and the 05th of September. The fluorometer was set up where the stream was narrow and deep at MP1, seen in figure 3.14. The dye was injected where the stream flowed out of the glacial lake, at IP1. The distance between the injection and the measuring point was 616,5 metres.

On August 31st 2016, background logging started at 11.07 from MP1. 50ml Rhodamine WT was injected into IP1 at 11.34. Logging continued until 14.24. Figure 3.16 shows the colour of the stream 100 meters from IP1, a couple of minutes after injection.

On September 05th o2016, we started logging background values from MP1 at 12.10, and injected 50ml Rhodamine WT into IP1 at 12.28. Logging continued until 14.52, when values were back to background level.

Figure 3.16 The dye concentration close to the injection points is clearly visible. The image also illustrates the typical width and depth of the proglacial stream. Photo: Jan Hedges

A third field measurement, "Lake #4," was performed, where we also passed the dye signal through the valley lake before it was measured. On September 21st 2016, the fluorometer was set up at the outlet of the valley lake, at MP4. The fluorometer started logging at 11.38, and 50ml of Rhodamine WT was injected into IP1 at 12.12. The fluorometer was left logging until the 23rd of September, when measurements were concluded at 10.10.

3.4.6 Supraglacial stream and glacial lake set up

Two field measurements were carried out in a supraglacial stream which ran on top of the glacier below IP3. The supraglacial stream appeared to enter the stream which exited the glacier before entering the glacial lake. One measurement, Supra-stream #6, was carried out with the fluorometer placed in the stream at MP2. The other, Supra-lake #5, was carried out with the fluorometer placed at MP3, which meant the dye signal would have to pass through the glacial lake.

On September 23rd, the fluorometer was set up at MP3 for Supra-lake #5 (this was done before the other measurement due to practical time constraints). The fluorometer started logging background values from MP3 at 10.43, and 100ml Rhodamine WT was injected at IP3 in the supraglacial stream at 10.56. The fluorometer was left logging until 15.58 on the 26th of September.

On September 27th, the fluorometer was set up at MP2 for Supra-stream #6. Background logging at MP3 started at 12.00. 100ml Rhodamine WT was injected at IP3 in the supraglacial stream one day later, on September 28th at 09.39 (this was because we did not bring the intended amount of dye on the 27th). The fluorometer was left logging until 10.48 on October 4th. Figure 3.17 shows the fluorometer set up at MP2, with the location of the supraglacial stream barely visible to the left of the large debris-pile on the glacier.

Figure 3.17 The fluorometer setup at MP2, directly below the glacier. The supraglacial stream can barely be spotted; it is located to the left of the large debris-pile in the upper right quadrant of the image. The dye was injected at IP3, which is located a short distance above the same large debris pile. Photo: Jan Hedges

4 Results and analysis

4.1 Diffusion

A - Results

In the lab experiment Diffusion #1, 10µl of Rhodamine WT was injection into the centre of a 1,54m long, thin volume of water. The fluorometer was placed at one end, and measured how the dye concentration changed over time as the Rhodamine WT diffused through the system.

The results have been plotted in figure 4.1, along with a simulation of the same experiment made using the numerical model. In the lab, the fluorometer first registered rhodamine WT after about 100 minutes. Then the concentration increased quickly until it reached a peak value of 592ppb after 330 minutes. Between 330 min and 400 min, there is a sudden drop in concentration, and from 400 min and onward the concentration remains relatively stable at about 500ppb. The simulation predicts that the concentration will increase at a lower rate from 70 minutes on, and level out at a concentration of 505 ppb.

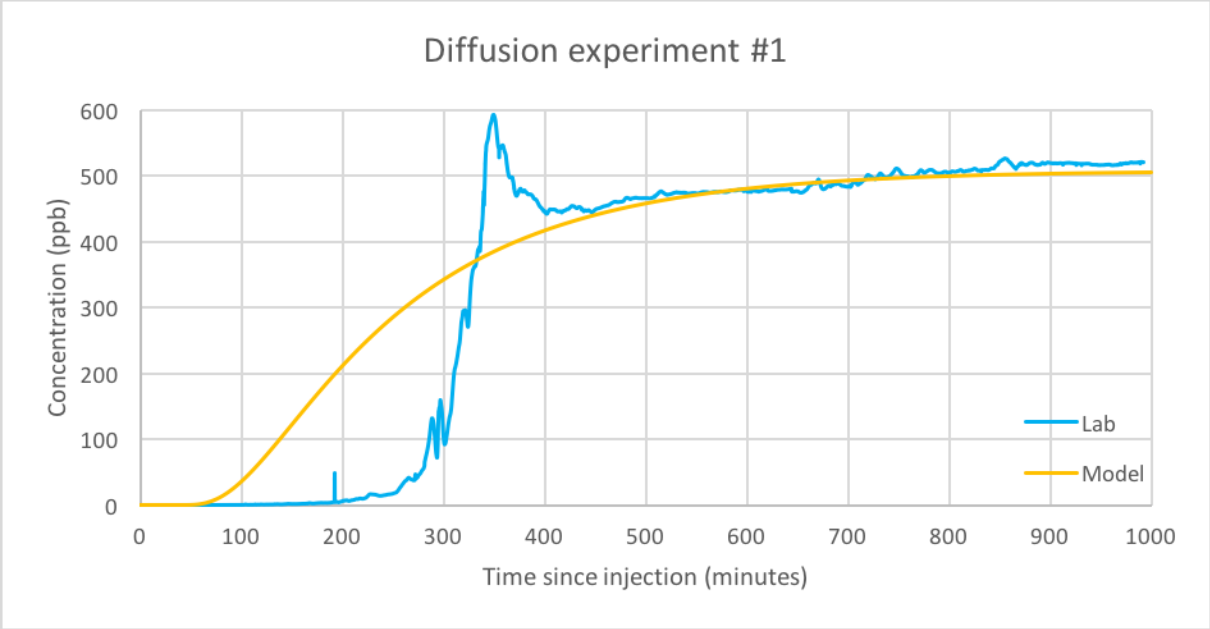

Figure 4.1 The breakthrough curve from the lab Diffusion #1 experiment is shown in blue. A simulation of the same experiment using the numerical model is plotted in yellow. While the initial concentration increase occurs more quickly in the lab than in the model, they both flatten out at about 500 ppb.

The second lab experiment, Diffusion #2, used the same set up but this time with the fluorometer placed in the middle of the system, just 15 cm from the dye injection. The results have been plotted in figure 4.2, along with a simulation of the same experiment. The numerical model predicts that the concentration would steeply increase to 615 ppb in 120 minutes, then slowly decrease, and level out at a concentration of about 260 ppb. The lab

concentration reached a peak at 120 minutes, but the concentration of this peak was 100 ppb less than the model. The measured value then decreases, reaching its lowest value after 240 minutes. After this the graph evens out with a concentration between 200 ppb and 250 ppb. The lab experiment was ended after 1046 minutes.

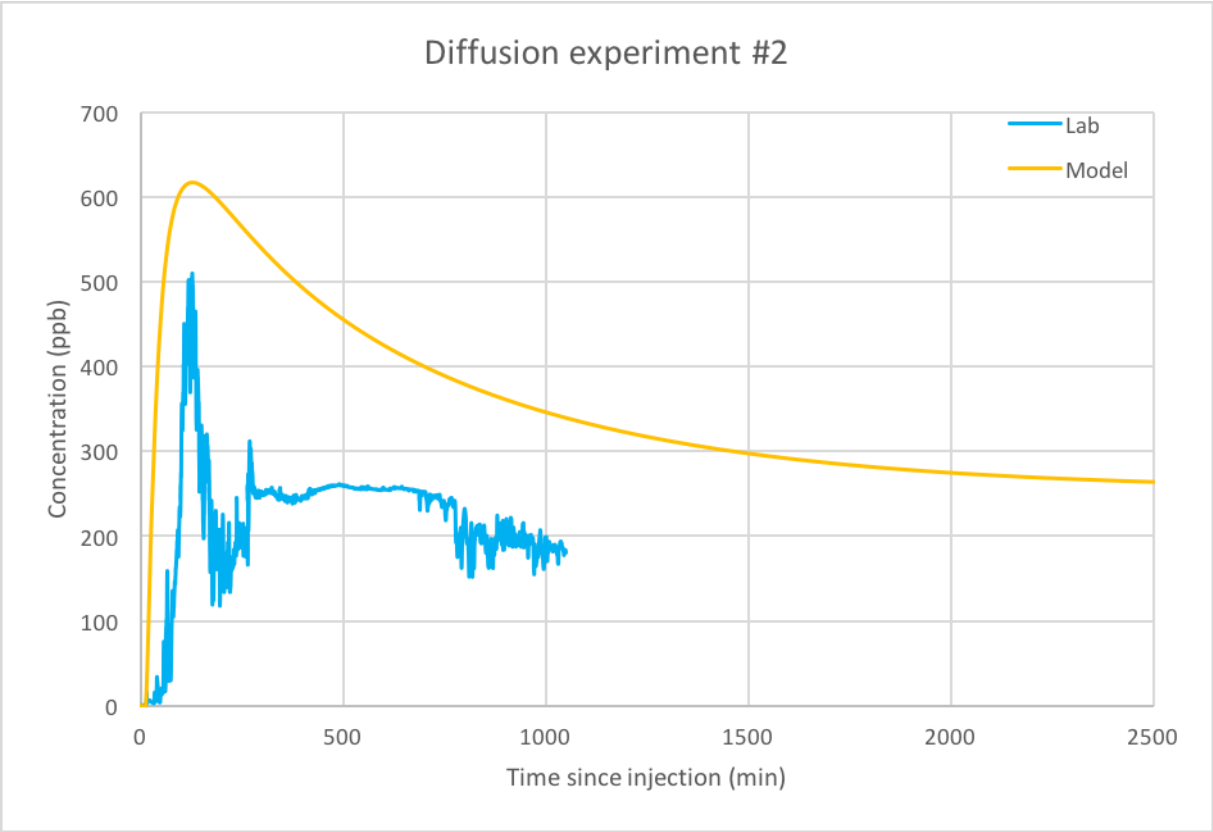

Figure 4.2 The breakthrough curve from the lab Diffusion #2 experiment is plotted in blue. A simulation of the same experiment using the numerical model is plotted in yellow. The timing of the peak concentration is the same in the lab experiment as in the simulation, although the concentration amount is not the same.

B – Analysis

The diffusion experiments are dominated by a lot of fluctuations and abrupt changes in ppb concentrations. In Diffusion #1 (figure 4.1) the measured and modelled concentrations even out at about the same concentration. Other than that, the model predicts a smoother increase in ppb than the lab experiment showed. In Diffusion #2 (figure 4.2) the model predicts a peak at a higher value than measured, and a lot longer time to even out throughout the system. Both measurements indicate a diffusion coefficient of ~$6*10^{-6}$ m^2/s, which is used in the model. Compared to the diffusion coefficient for Rhodamine B of $4{,}27\pm0{,}04*10^{-10}$ m^2/s (Gendron, Avaltroni, & Wilkinson, 2008), the experiment diffuses a lot quicker than expected. This is discussed in section 5.1.

4.2 Lab experiments

4.2.1 Lab calibration results

We performed numerous calibrations in the lab; a summary is shown in figure 4.3. Calibration #2 was our first dataset, but did not include the high gain range. Calibration #3 spans the entire low, medium and high gain ranges. Both of the wider datasets had poor resolution in the low gain range. Since most of our actual lab experiment measurement results have very low concentrations, calibration #4 and #5 were conducted to increase the resolution in the low gain range.

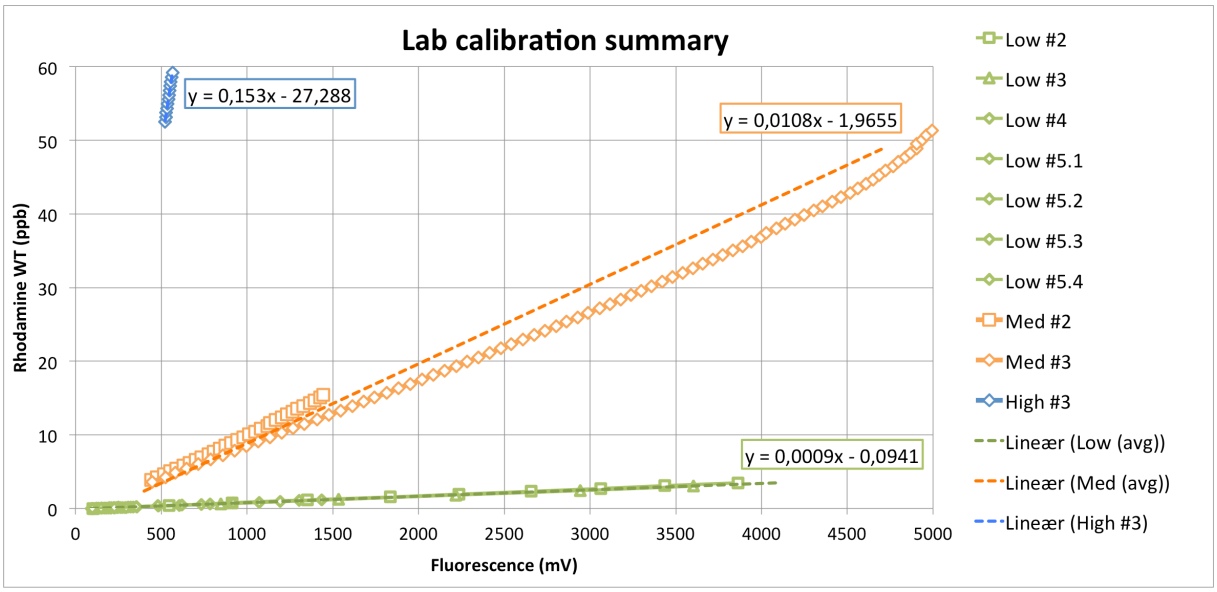

Figure 4.3 An overview of the multiple lab calibrations that were used to determine the relationship between measured fluorescence (mV) and dye concentration (ppb). Each data point represents a calibration step. The equations (mV(x) to ppb(y)) are shown next to their corresponding calibration curves.

To generate the mV to ppb equations, linear regressions were done on the calibration data sets for each gain setting. The resulting equations are also shown in figure 4.3. The low gain data set consists of seven independent calibrations, and the linear regression is performed on an average of these calibration curves. In the medium gain range, Calibration #3 spanned the entire medium gain range, but was slightly curved. Calibration #2 had a smaller data spread, but completely linearity within its data. The equation for the medium gain setting was generated by taking the linear regression on the average of these two calibrations. The high gain equation is based solely on a linear regression of the high gain data points from Calibration #3.

4.2.2 Siphon experiment results and analysis

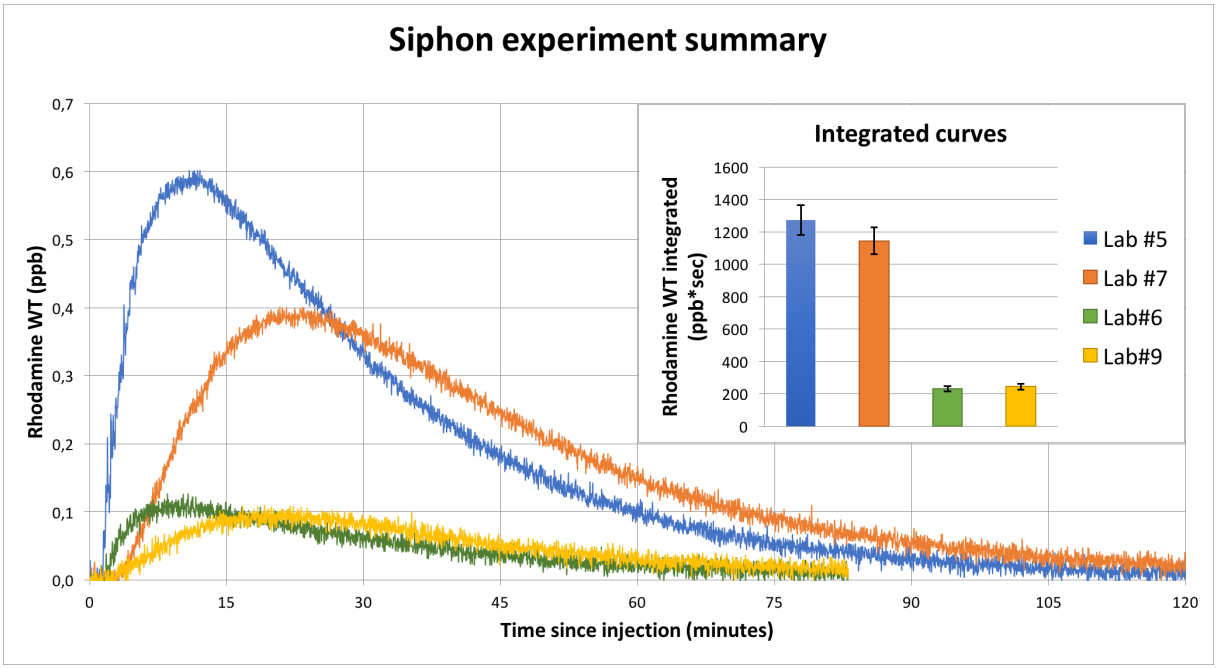

Figure 4.4 Breakthrough curves from the four measurements performed during the siphon experiment. Also shown are the integrated values for each curve. Lab #5 and #7 had the same volume dye injections, but were injected at different points along the system. The same was done for Lab #6 and #9, with less dye. For detailed information see table 2.

In the four siphon experiment measurements, we varied the dye volume and injection points to see how this would affect the breakthrough curves and the estimated discharge. The breakthrough curves and integrated values from the siphon experiments are shown in figure 4.4. The shapes of the breakthrough curves indicate that the lateral mixing is satisfactory; the peaks are rounded and they have a long falling limb. When integrated, the areas are similar for breakthrough curves where the same dye volume was injected at different injection points. Equation 11 was used to estimate the discharge (Q) from the integrated curves. The Q values that have been estimated by equation 11 are close to the actual Q value during the experiment. In all four cases, the estimated Q value is larger than the actual Q value. All the values are shown in table 2.

Table 2. Shows the parameters used in the siphon experiment, the measured results, and the estimated Q (using equation 11).

Measurement number	Volume of dye (µl)	Injection point	Area under curve (ppb*sec)	Measured Q (L/min)	Estimated Q (L/min)
Lab #5	1,0	Midstream	1272,55	1,0	1,084
Lab #7	1,0	Upstream	1144,35	1,0	1,206
Lab #6	0,2	Midstream	232,10	1,0	1,189
Lab #9	0,2	Upstream	244,15	1,0	1,130

4.2.3 Stream and basin experiment results and analysis

The stream and basin experiment was performed multiple times in various configurations, as described in section 3.3.1. The results have been summarized in table 3. Note that each of the measurements from Lab #12, #13 and #14 are based on the average of five repeated measurements with the same conditions.

Table 3. This table lists the results from the stream and basin experiment, and the actual and estimated Q values from each measurement. The naming scheme reflects the volume of 1/50000 dilution of Rhodamine WT that was injected. Note the negative discharge values estimated by the two lowest volume injections in the Lab#15 experiment.

Measurement number	Volume of dye (µl)	Area under curve (ppb*s)	Actual Q (L/min)	Estimated Q (L/min)
Lab #12(1ml)	0,20	82,75	7,90	3,50
Lab #12(250µl)	0,05	8,56	7,90	8,47
Lab #13(1ml)	0,20	136,33	7,90	3,08
Lab #13(250µl)	0,05	7,86	7,90	9,31
Lab #14(1ml)	0,20	99,39	4,55	2,92
Lab #14(250µl)	0,05	17,38	4,55	4,17
Lab #15(1ml)	0,20	87,17	3,64	3,53
Lab #15(250µl)	0,05	26,62	3,64	2,59
Lab #15(100µl)	0,02	9,28	3,64	3,12
Lab #15(50µl)	0,01	2,47	3,64	5,86
Lab #15(25µl)	0,005	*-1,04*	3,64	*-6,99*
Lab #15(10µl)	0,002	*-1,04*	3,64	*-2,78*

In the stream measurements (Lab #12, #13 and #14) the 250µl injections give noticeably more precise estimates for Q than the 1ml injections. In the stream and basin measurements (Lab #15) the precision of the estimated Q varies between dye injections. For the smallest volumes of dye, the estimate for Q is negative, indicating backwards flow. The negative estimate occurs when the area under curve (A_c) is calculated to be negative. The A_c has a chance of becoming negative when the breakthrough curve is so weak that the random fluctuations in background fluorescence is stronger than the actual dye signal.

4.3 Field results

4.3.1 Field calibration results

During our field trips we did three calibrations. The first one turned out to have insufficient mixing time between steps and was not suitable for calibration, while the data from another calibration was lost to an untimely DataBank reset. Fortunately, the one remaining calibration turned out to have good mixing between steps and linearity within gain settings, as seen in figure 4.5.

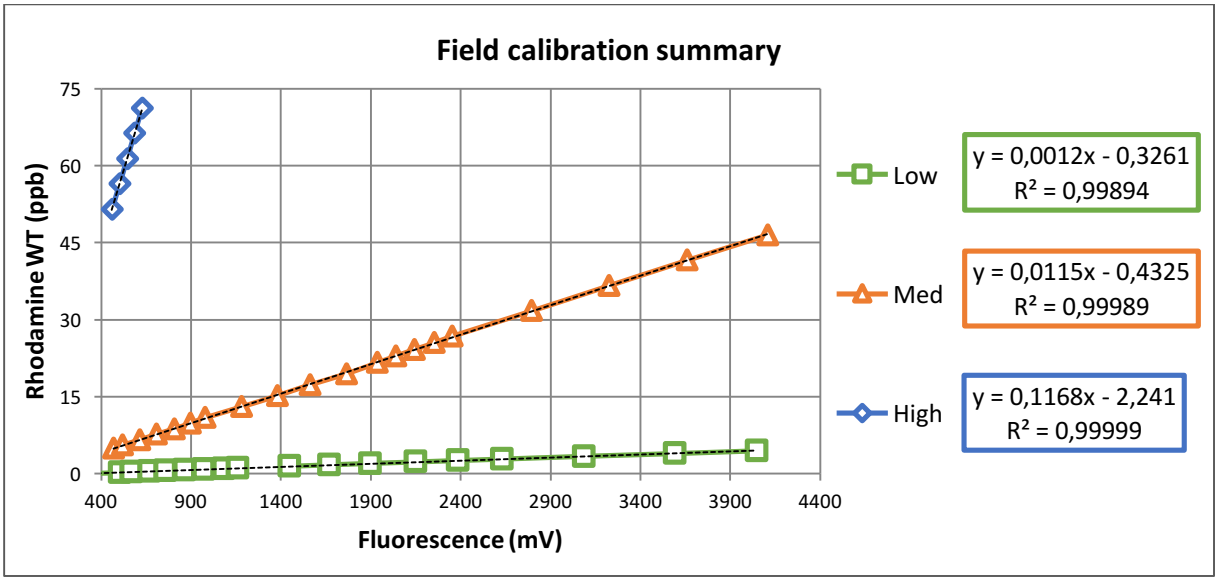

Figure 4.5 A plot of the calibration curves used for transforming mV values into Rhodamine WT concentration with linear equations. Each data point represents a calibration step. The equations (mV(x) to ppb(y)) are shown in boxes next to their gain settings.

Some error correction was applied to preserve the linearity of the calibration curves. We removed one data point in the low gain range, which showed a one-time decrease in mV when dye was added. We also detected a sudden jump (>250% of the mean step increase) at the 20-21 ppb step within the medium gain range. This jump occurred just after an addition of pure Rhodamine WT had been made into the solution bucket (1). We interpreted this to imply that in the following calibration step, some unaccounted for amount of Rhodamine WT got into the calibration bucket (2), either via the pipette, stirring spoon or other mishandling of equipment. The measurements returned to linear after the one-time ppb jump. We removed the additional fluorescence (266 mV) from all subsequent measurements, and accounted for the transition from medium to high gain by keeping the relationship constant between the last medium gain reading and the first high gain reading. After the error corrections, we applied a linear regression model to the calibration curves for each gain setting, to get our equations for turning mV values into dye concentrations in ppb. The equations are shown in figure 4.5.

4.3.2 Proglacial stream measurement

In field measurements Stream #1 and Stream #2, 50 ml of Rhodamine WT dye was injected in the proglacial stream below Skjerdingane cirque glacier, while the dye concentration in the water was measured by a fluorometer placed 616,5 m downstream. The return curves from both measurements can be seen in figure 4.6.

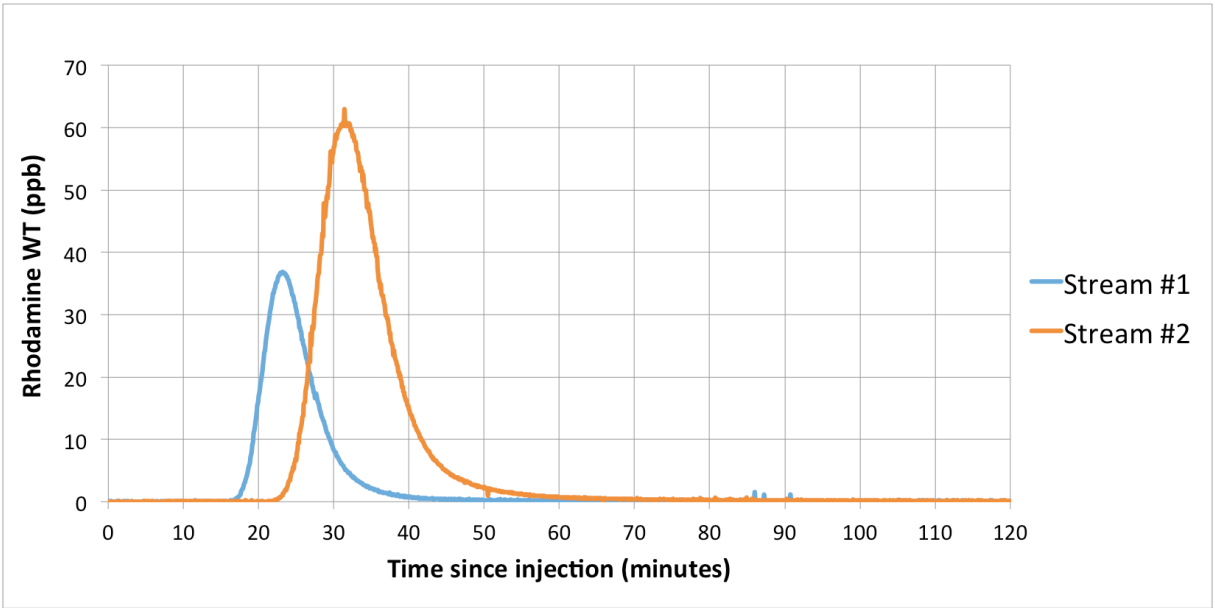

Figure 4.6 The Rhodamine WT breakthrough curves from the Stream #1 and Stream #2 measurements performed in the proglacial stream in Skjerdingane. The difference in size reflects the different discharges at the time of measurement.

The breakthrough curves have been integrated, and dye trace parameters have been estimated using equation 11, giving the values listed in table 4. The breakthrough curve from Stream #2 is more than twice the size of the breakthrough curve from Stream #1, taken just five days prior. The stream flow on 31.08 was visually observed to be high, and there was a lot of rain on the morning before the measurement was taken. On 05.09, there had been a dry spell, and the stream flow was visibly reduced. This is reflected in the Q and A_{sm} values estimated by analysing the breakthrough curves.

*Table 4.*Lists the time and precipitation for the field measurements on the proglacial stream and valley lake in Skjerdingane. Also listed are the dye trace parameters calculated using equation 10, 11 and 12.

Measurement number	Date	Rain (mm)	V_i (ml)	A_c (ppb s)	Q ($m^3 s^{-1}$)	u ($m s^{-1}$)	A_{sm} (m^2)
Stream #1	31.08.16	13,0	50	18578	0,62	0,45	1,39
Stream #2	05.09.16	0,3	50	40645	0,28	0,33	0,87
Lake #4	21-23.09.16	3,2	50	39822	0,29	0,14	2,04

4.3.3 Valley lake measurement

In the stream and lake measurement, Lake #4, 50ml of Rhodamine WT dye was injected at the same location (IP1) as in the Stream measurements, while fluorometer was set up below the valley lake (MP4). The breakthrough curve from Lake #4 is plotted in figure 4.7, along with temperature data from Anestølen and Frudalen (NVE, 2016b), and precipitation data from Selseng (NVE, 2016a).

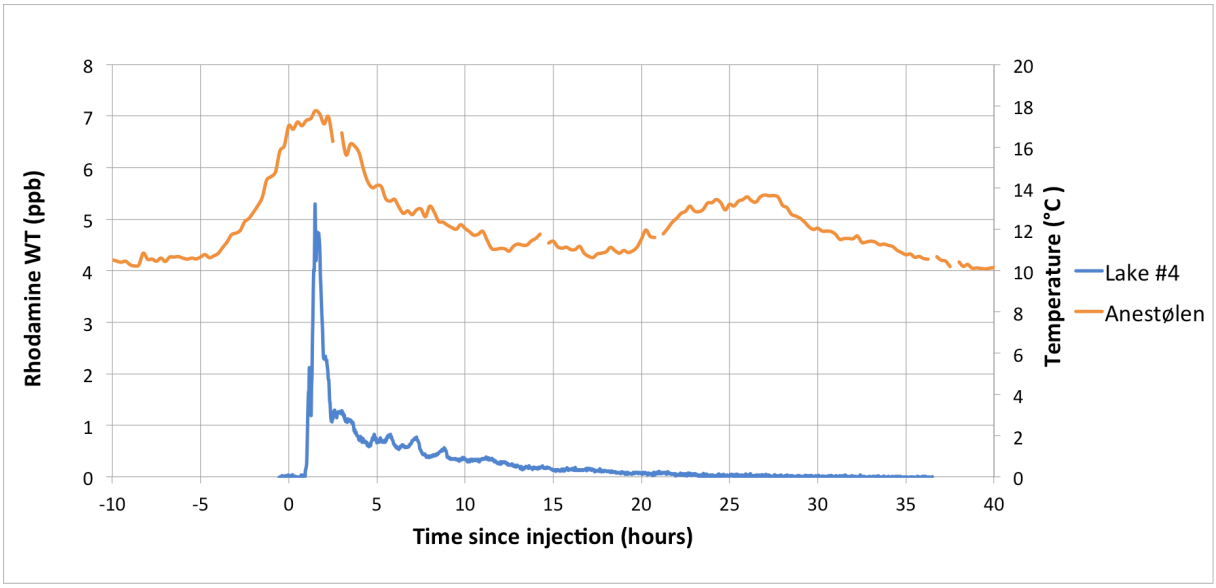

Figure 4.7 Breakthrough curve for the Lake #4 measurement in blue, plotted alongside temperature data from the weather station at Anestølen (NVE, 2016b). No detectable increase in fluorescence is observed at the second temperature peak at 25 hours.

The breakthrough curve has been elongated to last 30 hours (where the breakthrough curve from Stream #2 lasted 30 minutes), yet it is still clearly recognizable. There is a temperature peak concurrent with the fluorescence peak at 2 hours. A second temperature peak at 25 hours produces no discernible increase in fluorescence. The breakthrough curve has been integrated and parameters have been calculated and shown in table 4. The discharge is unchanged from Stream #2, while stream velocity and average channel width have decreased.

4.3.4 Glacier measurements

A - Results

In field measurement Glacier #2, we injected 50ml of dye at the back of the glacier and set up the fluorometer in the glacial stream entering the glacial lake. The resulting time-concentration curve can be seen in figure 4.8, where it has been plotted alongside temperature

measurements from the weather stations in Frudalen and Anestølen (NVE, 2016b).

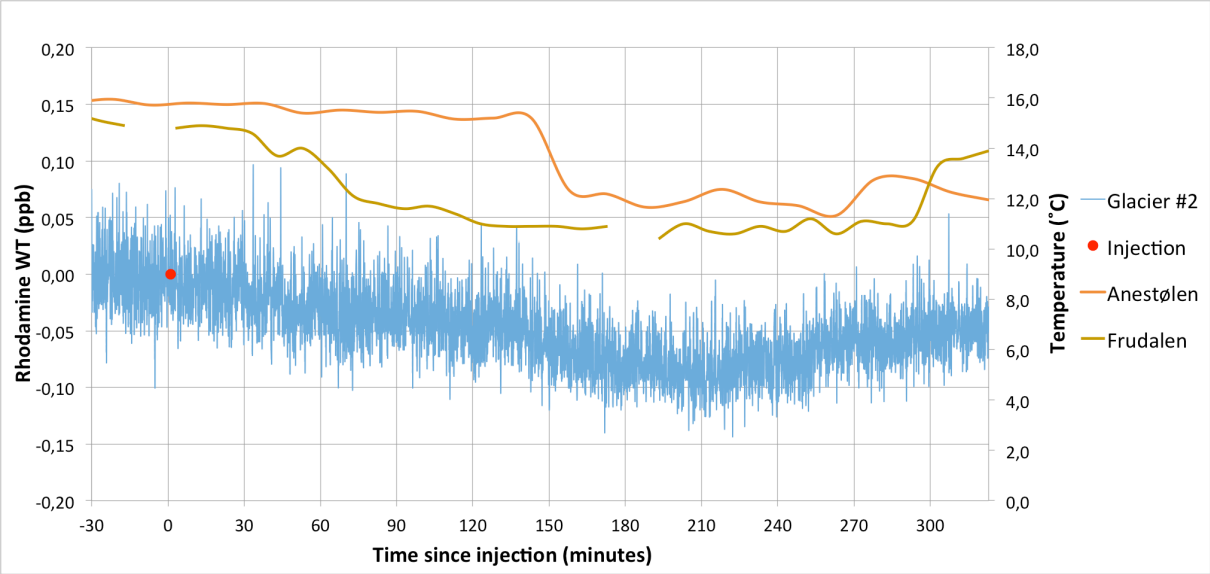

Figure 4.8 The time-concentration curve of the Glacier #2 measurement, as well as temperature data from weather stations in the area (NVE, 2016b). No increase in fluorescence above background levels is observed after the dye is injected.

In field measurement, Glacier #3, we injected 50ml of dye at the back of the glacier. This time we put the fluorometer at the outlet of the glacial lake and the measurement lasted for over three days. The time-concentration curve from this experiment can be seen in figure 4.9, where it has been plotted alongside temperature measurements from Frudalen and Anestølen (NVE, 2016b).

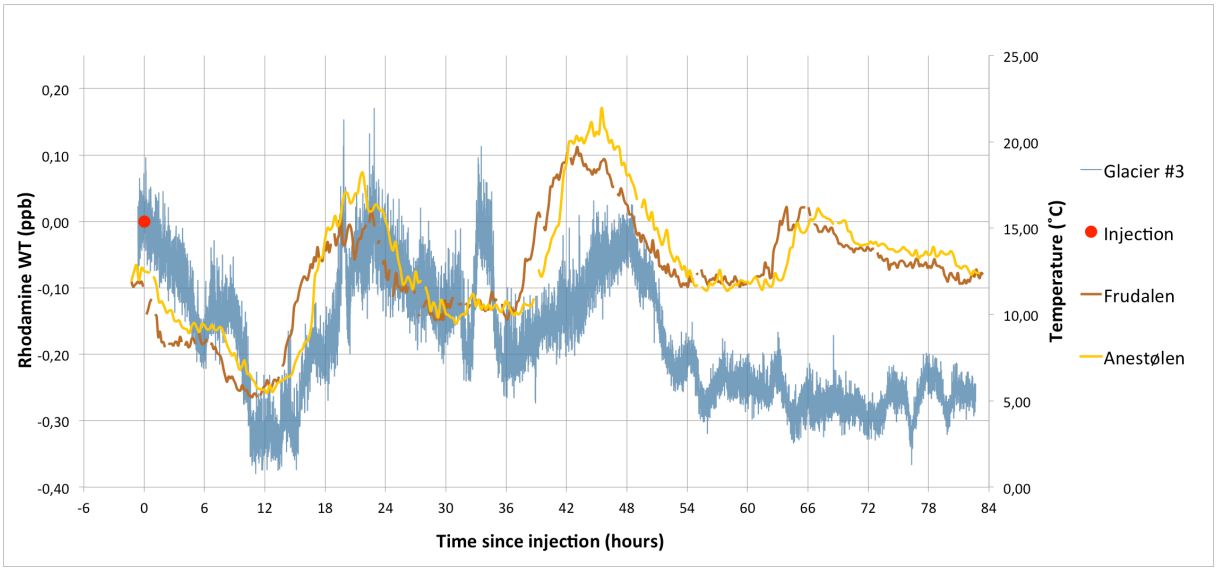

Figure 4.9 Shows the time-concentration curve of Glacier #3, as well as temperature data from weather stations in the area (NVE, 2016b). No increase in fluorescence above background levels is observed after the dye is injected. fluctuations appear to have an impact on the background fluorescence.

B - Analysis

Both glacier measurements show an overall decrease in average fluorescence after the dye is injected. In Glacier #3 there are larger variations, due to the fact that this was left logging over a considerably longer time period. There appears to be a connection between air temperature and the fluorescence in the stream. Warm temperatures like the ones in Glacier #3 will cause extensive melting of the glacier, which will increase water flow in the stream, which in turn will increase the amount of suspended sediments (Benn & Evans, 2014). Suspended sediments like silt have been shown to increase fluorescence (Smart & Laidlaw, 1977).

4.3.5 Supraglacial stream and glacial lake measurements

In Supra-lake #5 and Supra-stream #6, we performed two measurements in a supraglacial stream flowing from on top of the glacier, and into the stream exiting the glacier. 100ml of dye was injected at IP3, and breakthrough curve was measured both before and after passing through the glacial lake. For Supra-stream #6, the fluorometer was set up at MP2, in the stream between the glacier and the glacial lake. For Supra-lake #5, the fluorometer was set up at MP3, below the outlet of the glacial lake.

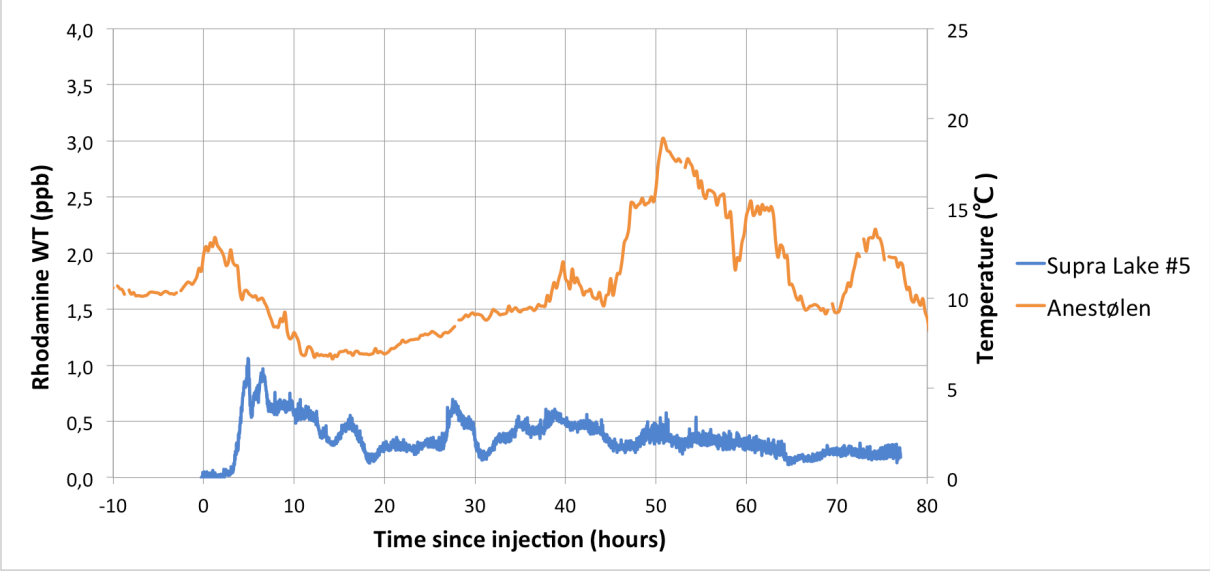

Figure 4.10 Shows the breakthrough curve for Supra-lake #5, alongside temperature data from the weather station at Anestølen. The tail end of the breakthrough curve may have been affected by the temperature peak at 50 hours.

A - Results

The breakthrough curve from Supra-lake #5, seen in figure 4.10, show low, yet stable concentrations over a long time-period. When we ended the experiment, the fluorometer had been logging for 76 hours, and still had not reached initial background values.

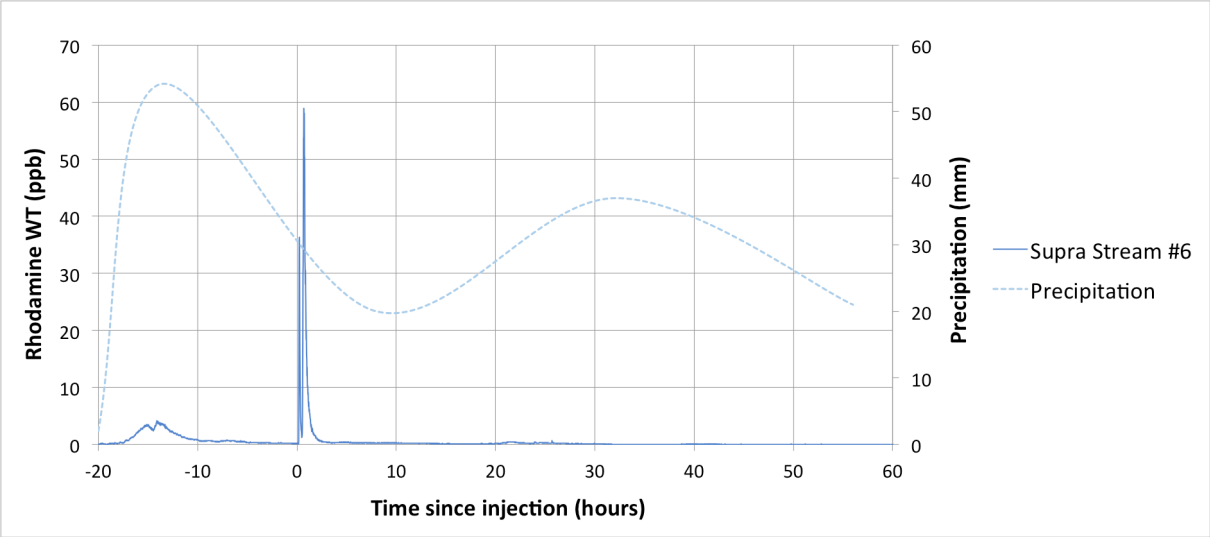

Figure 4.11 The breakthrough curve from Supra-stream #6, which is the very steep peak that appears shortly after the dye is injected at hour 0. This is plotted alongside precipitation data from the weather station at Anestølen. Another fluorescence peak is also seen, appearing 15 hours *before* the dye injection.

The breakthrough curve from Supra-stream #6, seen as the very steep peak in figure 4.11, appears 10 minutes after dye injection. Another fluorescence peak is present at -15 hours, appearing *before* any dye has been injected.

B - Analysis and discussion

Supra-lake #5

The temperature peak at 50 hours during Supra-lake #5 might have caused an increase in the fluorescence, making it hard to determine the exact shape of the breakthrough curve. Based on background readings from the same fluorometer placement in the Glacier #3 measurement, we might except a slight increase (about 0,3ppb) in background fluorescence caused by the warm period at 50 hours.

Supra-stream #6

Regarding the unexpected fluorescence peak at -15 hours in Supra-stream #6, we will present our theory for why it occurred as it highlights a potential error source in other fluorometric investigations. At the start of Supra-stream #6, the fluorometer was set up and logging background values for twenty hours; from 12.00 on the 27th to 09.40 on the 28th of September At 09.40 on the 28th, the 100ml dye injection was made. Supra-stream #6 was performed in the same supraglacial stream where Supra-lake #5 had been performed just a few days prior. In this supraglacial stream, there were several small stagnant pools in the glacier ice along the

side of the stream. Between dye injection for Supra-lake #5 and up until right before the appearance of the unexpected fluorescence peak, there had been a dry period with almost no precipitation. On the evening of the 27th, just before the fluorescence peak shows up, it began raining heavily. Our best guess is that some quantity of the dye injected for the Supra-lake #5 measurement remained stranded in stagnant water along the supraglacial stream. During the heavy rain on the 27th, this leftover dye could have been washed into the stream and produced the fluorescence peak seen at -15 hours.

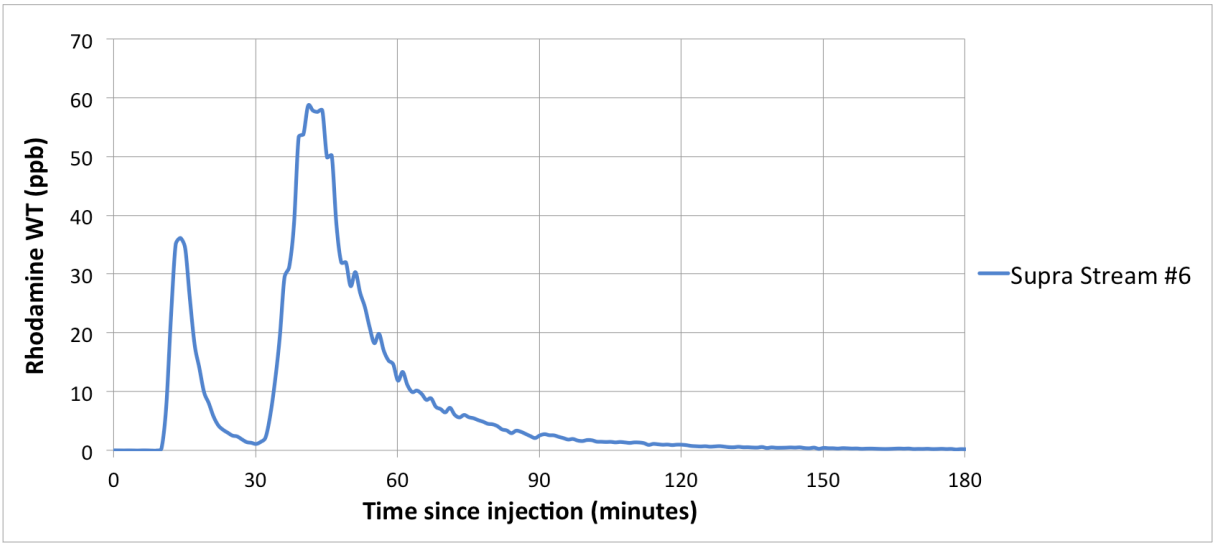

Figure 4.12 Close-up of the breakthrough curve from Supra-stream #6, which shows two separate concentration peaks.

Figure 4.12 shows a close-up of the actual breakthrough curve from Supra-stream #6. The two concentration peaks could indicate that the water in the supraglacial stream splits off into two different paths at some point between the dye injection and the fluorometer. Based on breakthrough curve analysis, we can calculate some parameters of these peaks, as seen in table 5.

Both breakthrough curves have a dispersivity (α) of less than 10. As described in section 2.2.5, this indicates that the breakthrough curves originate from well-developed streams. Peak 1 could then be further be assumed to pass through a more well-developed system than peak 2. In addition to the parameters in table 5, the overall Q of the two breakthrough curves combined is estimated to be 0,27 m^3/s.

*Table 5.*Lists the parameters for the two distinct concentration peaks in the Supra-stream #6 measurements, based on breakthrough curve analysis of each separate peak.

Measurement number	Time of travel (s)	Velocity u (m s^{-1})	Dispersion coefficient D (m^2 s^{-1})	Dispersivity α (m)
Peak 1	847	0,22	2,07	9,24
Peak 2	2467	0,08	0,62	7,99

4.4 Numerical modelling results

A - Results

The stream measurements from lab experiment #12, #13 and #14 and field stream #1 and #2 was replicated in the numerical model. With the aim of being able of estimating the measurements dispersion coefficients. Figure 4.13 presents the measured the mean value of the breakthrough curves from lab #12.6-12.10 where the stream was without sediments, #13.6-13.10 and #14.1-14.5 with added sediments, and the breakthrough curves of Stream #1 and #2.

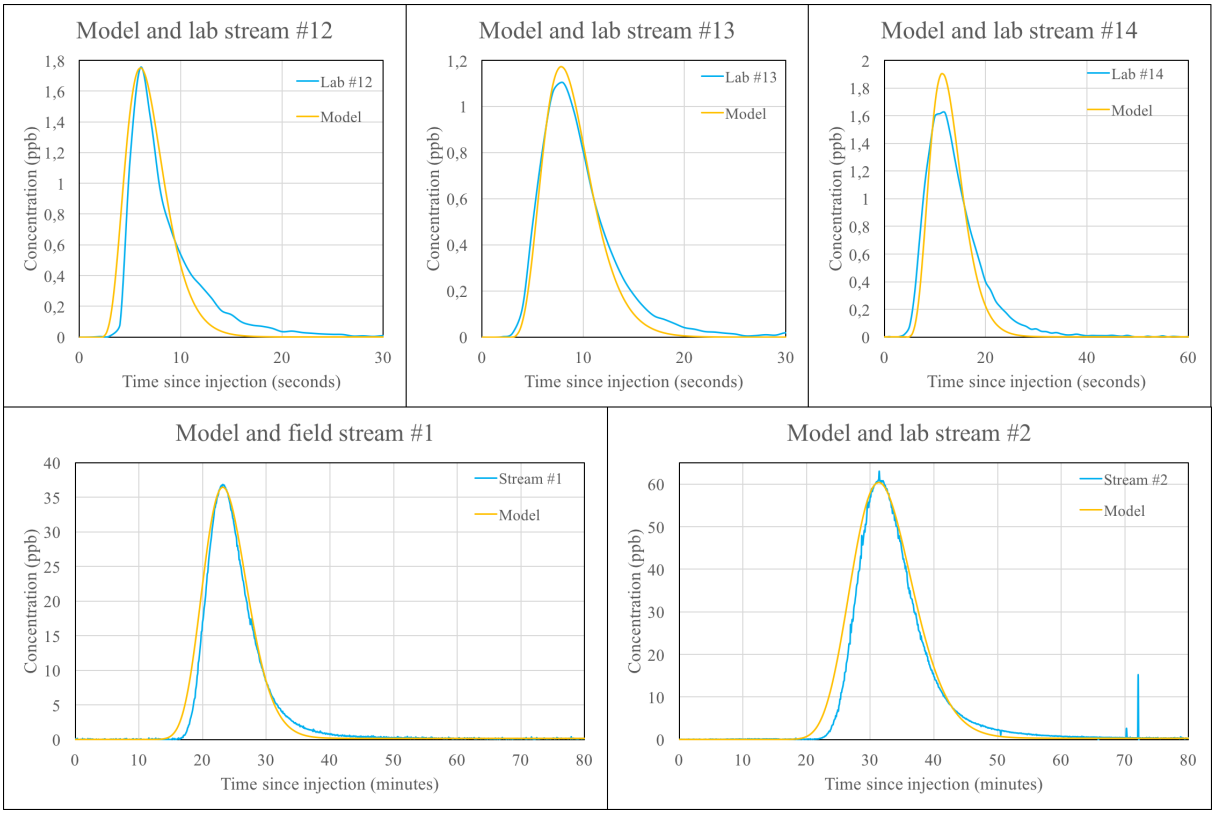

Figure 4.13 Breakthrough curves from lab #12, #13, #14, and stream measurement #1 and #2, shown in blue. They are plotted alongside simulations from the numerical model, which have been adjusted to fit the observed curves.

The measurement and model data are presented in table 6. The model parameters are presented in table 7.

Table 6. Lists measurement and model data from lab #12, #13, #14, stream #1 and #2. The data consists of Discharge (Q), amount of dye injected, peak concentration, peak time of measurements and model, and time for all dye to pass (time passed) the sensor, for the measurements and model.

Measurement number	Q (L/min)	Dye injected	Peak (ppb)	Model peak (ppb)	Peak, time since injection	Model peak time	Time passed	Model passed time
Lab #12	7,90	0,05 µl	1,75	1,71	6 sec	6,2 sec	30 sec	20 sec
Lab #13	7,90	0,05 µl	1,10	1,17	8 sec	7,7 sec	26 sec	20 sec
Lab #14	4,55	0,05 µl	1,62	1,90	12 sec	12 sec	40 sec	29 sec
Stream #1	18 000	50 ml	36,86	36,6	23 min 10 sec	22 min 43 sec	50 min	41 min
Stream #2	39 000	50 ml	62,87	60,5	31min 25 sec	32 min	84 min	55 min

Table 7 Model parameters used to simulate Lab #12, #13, #14, Stream #1 and Stream #2.

Measurement number	Δx (m)	Δt (s)	v (m/s)	K	Length (m)	D (m^2/s)
Lab #12	0,01	0,35	0,24	0,408	1,45	0,012
Lab #13	0,01	0,48	0,18	0,4224	1,45	0,0088
Lab #14	0,01	0,7	0,12	0,42	1,45	0,006
Field #1	10,0	21	0,445	0,28	615	2,0
Field #2	10,0	21	0,327	0,378	615	1,8

B – Analysis

Lab #12 did not have sediments in the stream, to see what difference a laminar flow had on dispersion compared to streams with a turbulent flow (lab #13 and #14 with sediments). The Reynolds number (equation 13) for Lab #12 was 836,4 indicating a laminar flow. Calculating Re for lab #13 and #14 is hard, as the sediments increased the wetted perimeter by an unknown amount (decreasing the value of Re), but also came up over the stream surface creating eddies in some areas.

The parameters in the models are manually adjusted to best fit the measured breakthrough curve of the lab and field measurements so that a value of D can be obtained. The D-values suggested by the model for experiment #12, #13, and #14 are D=0,0120 m^2/s, D=0,0088 m^2/s and D=0,0060 m^2/s. The dispersion coefficients calculated from equation (13) are D=0,0360 m^2/s, D=0,0255 m^2/s and D=0,0217 m^2/s respectively. For the field measurements, the modelled dispersion coefficients are D=2,3 m^2/s for measurement #1 and D=1,8 m^2/s for measurement #2. The calculated dispersion coefficients (equation (13)) are D=10,098 m^2/s and D=7,235 m^2/s respectively. These results will be further discussed in chapter 5.1.

5 Discussion

5.1 Numerical modelling

5.1.1 Model reliability

From the diffusion experiment (section 4.1), the numerical model manages to replicate the rough outline and final ppb values of the measured diffusion curves. The diffusion coefficient predicted by the model is a lot higher than the diffusion coefficient stated for Rhodamine B. This is probably because there was some movement in the water during the diffusion experiments. This movement could be caused by convective currents induced by temperature gradients and evaporation. The convective currents make the rhodamine mix with the water quicker than if diffusion was the only process.

The model has been manually adjusted to replicate the shape, size and values of the measured breakthrough curves of Lab #12, #13, #14 and Stream #1 and #2. The elongated tales of the measured breakthrough curves are not replicated in the model, as shown in section 4.4-B

The intention was to use the models' diffusion coefficient as the breakthrough curves dispersion coefficient. As shown in table 8, the modelled diffusion coefficients are far from the calculated dispersion coefficients. The difference between the two values have a ratio of between 0,35 and 0,02.

Table 8. Lists the dispersion coefficients (D) from the numerical model, and the dispersion coefficients (D) estimated by equation (15). The final column lists the ratio between the values from the model and from the equation.

	Modelled D	Calculated D of modelled curve	Ratio (Model/Calculated)
Lab stream #12	0,0120	0,0340	0,35294
Lab stream #13	0,0088	0,4300	0,02047
Lab stream #14	0,0060	0,1480	0,04054
Field stream #1	2,0000	11,5000	0,17391
Field stream #2	1,8000	8,8300	0,20385

5.1.2 Use of the model

The numerical model can be used to observe how different parameters affect the possesses of diffusion and dispersion. It could be used to estimate how breakthrough curves may look like after a set amount of dye is passed through a stream with a length and a velocity.

5.1.3 Further model investigations

One of the problems with applying the numerical model to simulate the diffusion experiments, was that in the experiment the dye had to diffuse in three dimensions. To mitigate the 1D to 3D differences, the dye could initially have been injected in a closed section of the gutter. with barriers to allow dye to diffuse in a small cell. When fully diffused in the cell, the barriers could have been carefully removed, allowing the diluted rhodamine WT to diffuse lengthwise. This would closer resemble a one-dimensional system.

The model was intended to inspect what larger slow-moving bodies of water does to a breakthrough curve. Before this can be achieved, the discrepancy between the value of the diffusion coefficient used in the numerical model and the dispersion coefficient found using equation 14, must be understood. However, a review of the different empirical methods for obtaining the dispersion coefficient from experimental data is beyond the scope of this thesis.

5.2 Stream discharge measurements

5.2.1 Test of reliability in lab

To explore how our calculated values for discharge (Q = average flow) vary under different circumstances, we used equation 11 to estimate Q in a series of lab experiments where we could also directly measure the actual Q. A comparison of these two data sets can be seen in figure 5.1. It appears that equation 11 is producing somewhat accurate estimates for Q in our controlled lab experiments (R^2=0,69). Two of the lowest dye volume Lab#15 basin measurements, which produced negative Q values, have been removed. The Lab#12-14 measurements carried out with 1ml injections had very sharp breakthrough curve peaks, consisting of only one data point, which might indicate poor mixing conditions. When these three measurements are excluded from the linear model in figure 5.1, the R^2 value increases to 0,91, indicating a good fit by the estimated Q values.

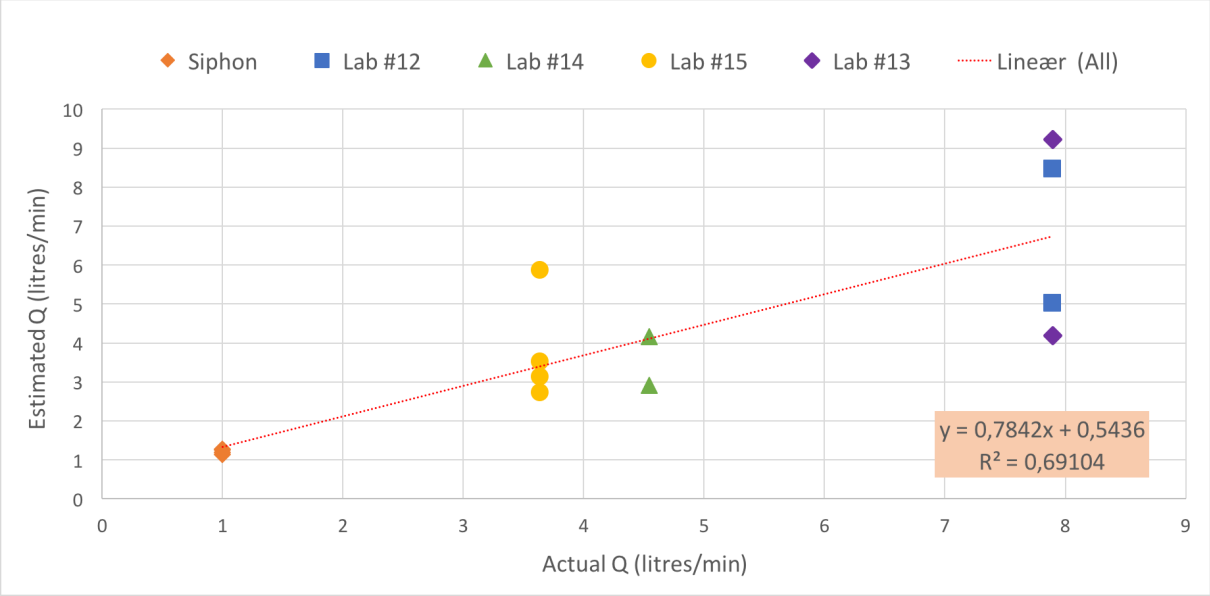

Figure 5.1 This scatterplot shows estimations of discharge from most of our lab experiments. They have been plotted against the actual discharge values, measured by stopwatch, from the same experiments. The linear regression shows how close our estimated Qs is to the actual Qs.

5.2.2 Estimates of field discharge in the proglacial stream in Skjerdingane

From the field measurements Stream #1 and Stream #2 we have calculated the discharge, or average flow (Q, m^3 s^{-1}), by integrating the breakthrough curves and using equation 11. The estimated values for Q can be seen in figure 5.2.

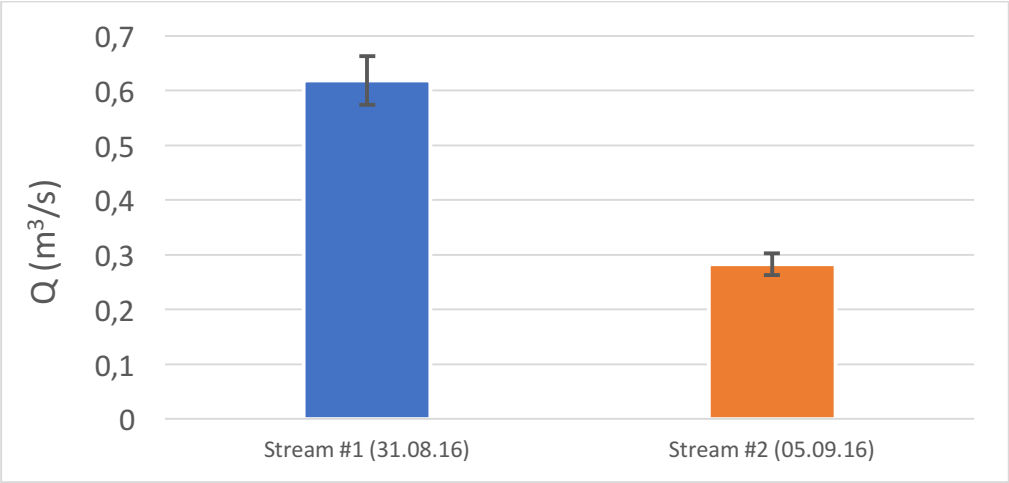

Figure 5.2 Shows the estimated discharge (Q, m^3 s^{-1}) in the proglacial stream in Skjerdingane at two different times during the melting season of fall 2017.

These values represent the discharge of the proglacial stream below the Skjerdingane cirque glacier on August 31st and September 5th during the melting season of 2016, estimated by dye tracing studies. The Q values represent an average of the discharge over the duration of the measurements. The discharge will vary depending on time of day and meteorological conditions.

5.2.3 Discussion of error sources

The quantifiable sources of error can be found by looking at equation 11 ($Q = S_i V_i C_i / A_c$). The specific gravity of the dye (S_i), is constant. The volume of dye (V_i) is directly affected by the error margin of the pipette used to measure up the dye. The initial concentration of the undiluted dye (C_i) can vary with every batch produced (Fyffe, 2013), but no values have been supplied by the manufacturer at the time of writing. Finally, the area under the breakthrough curve (A_c) is affected by the error in the calibration used to convert fluorescence values (mV) into dye concentration (ppb) values. The calibration relies on both precise pipetting, and the water volumes in the two calibration buckets. Combined, there is a ±1% variation in the pipette used to measure V_i, and a ±6,2% variation in the calibration used to estimate A_c. This results in Q having an error margin of ±7,2%, shown in figure 5.2.

There are also multiple error sources that are harder to quantify. A potentially large error source is adsorption of dye onto sediments in the stream, which can result in dye recovery of Rhodamine WT as low as 45% in mountain streams (Bencala et al., 1983). Another large error source is both the in- and outflow of water between the injection point and the measuring point, which we have observed to be occurring at the stream in Skjerdingane. Error might also be introduced if there is unsatisfactory lateral mixing. Furthermore, there is the possibility that the measurements were ended too soon, resulting in the tail end of the breakthrough curve not being fully recorded.

5.2.4 Suggestions for improved discharge estimates

It would be hard to precisely estimate the in- and outflow of water between the injection and measuring points. There is a lot of snow cover and rock talus hiding potential stream branches, and the moraine deposits in the valley could also potentially both supply and remove water from the stream through groundwater flow. To estimate the grade of lateral mixing, one could use two (or more) fluorometers placed at different points along a cross-section of the stream. If the areas under the different breakthrough curves do not vary, this would indicate that the mixing is sufficient. To ensure that the entire breakthrough curve is recorded, it is important to gather extensive background readings before dye injection, and to keep the measurement going until the fluorescence returns to the recorded background level.

5.3 Lack of signal in glacier measurements

5.3.1 Glacier #2

The initial aim of the field work was to investigate the subglacial drainage system of the Skjerdingane glacier. This would be done by measuring a breakthrough curve from a dye injection passing through the glacier. As seen in figure 5.3, there is a sizeable stream at MP2, which exits the glacier below our injection point IP2, before it enters the proglacial lake. We tested our assumption that this stream was a main outlet for the glacier, by carrying out field measurement Glacier #2, which yielded no detectable signal.

Figure 5.3 Shows the fluorometer set up at MP2, and gives a visual on the flow conditions in the stream coming out of the glacier.

5.3.2 Glacier #3

The lack of a detectable signal in Glacier #2 indicates that the water flow from IP2 takes a different route through the glacier than we first assumed (roughly indicated in figure 5.4), or that it takes a much longer path than expected, leading to a drop in concentration to background levels before it reaches the fluorometer. The reason could be that water from IP2 either enters the proglacial lake directly somewhere beneath the glacier, or that it enters the groundwater flow in the moraine sediments beneath the glacier. To test this assumption, we set up field measurement Glacier #3, with the fluorometer set up at the outlet of the glacial lake (MP3). This way we could be sure that the dye would have to pass by the fluorometer at some point, assuming it entered the glacial lake at all. After 83 hours and 16 minutes of logging, we were not able to detect any signal from the background noise. The lack of signal in Glacier #3 indicates that either we used a too small volume of dye, or that the water from IP2 exits the cirque somewhere else, perhaps through groundwater flow. For various reasons, we were not able to repeat this measurement with more dye.

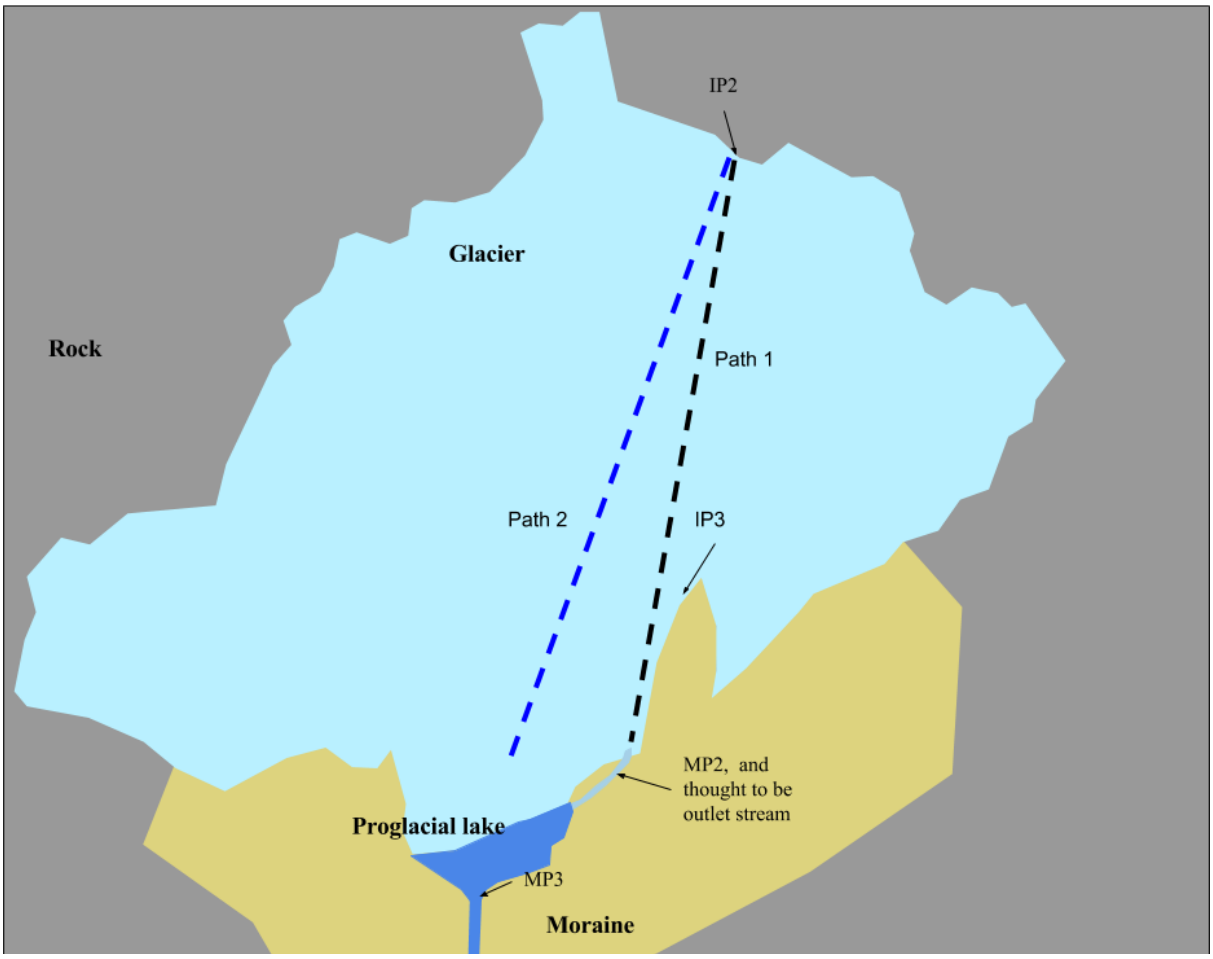

Figure 5.4 Sketch of the cirque glacier and surroundings of rock, moraine and proglacial lake. IP2, IP3, MP2 and MP3 are marked in the sketch. Path 1 indicates roughly our hypothesis of how water from IP2 would exit the glacier through the stream at MP2. Path 2 indicates a *possible* alternative path, which would deliver the water from IP2 directly into the proglacial lake.

5.3.3 Effects of the glacial lake

To better understand how dye signal from IP2 would be affected by passing through the glacial lake, we performed field measurements Lake #4 and Supra-lake #5, as well as lab experiment #15. The results from these measurements are discussed in section 5.3 below.

5.3.4 Further investigations

For future work, we would have liked to replicate the Glacier #3 measurement with a larger amount of dye (~500ml) injected at IP2 with the fluorometer set up at the outlet of the glacial lake. During our many trips to the glacier, we were unable to locate any suitable moulins. A moulin entering directly into the englacial drainage system would be more suited for dye injection than the mountain stream at IP2. As the glacier changes from season to season, it might be possible to locate a suitable moulin at a later time. Regarding the use of completely different methodology, a georadar with a depth sensitive antenna might be used to investigate the possibility of a subglacial lake influencing the hydrological system.

5.4 Effects of passing dye signals through large water volumes

5.4.1 Test of signal reduction in the lab

To investigate the effects on breakthrough curves that were passed through large volumes of water, we set up lab experiment #13 #14 and #15, which are described in detail in section 3.3.3. Breakthrough curves for different dye concentrations were measured before and after the dye cloud was passed through a large water volume. In Lab #15, increasingly small volumes of dye were injected and passed through the water volume until the signals were undistinguishable from background levels, as seen in figure 5.5. In our controlled lab experiment, we were able to statistically detect the breakthrough curve, using a Students t-test, even at very low concentrations (< 0,04 ppb). Detection was no longer possible when less than 0,01 µl of Rhodamine WT was injected into the flow (with parameters: Q = 2,7 litres per minute, total stream distance 1,85 m and water volume = 28 litres).

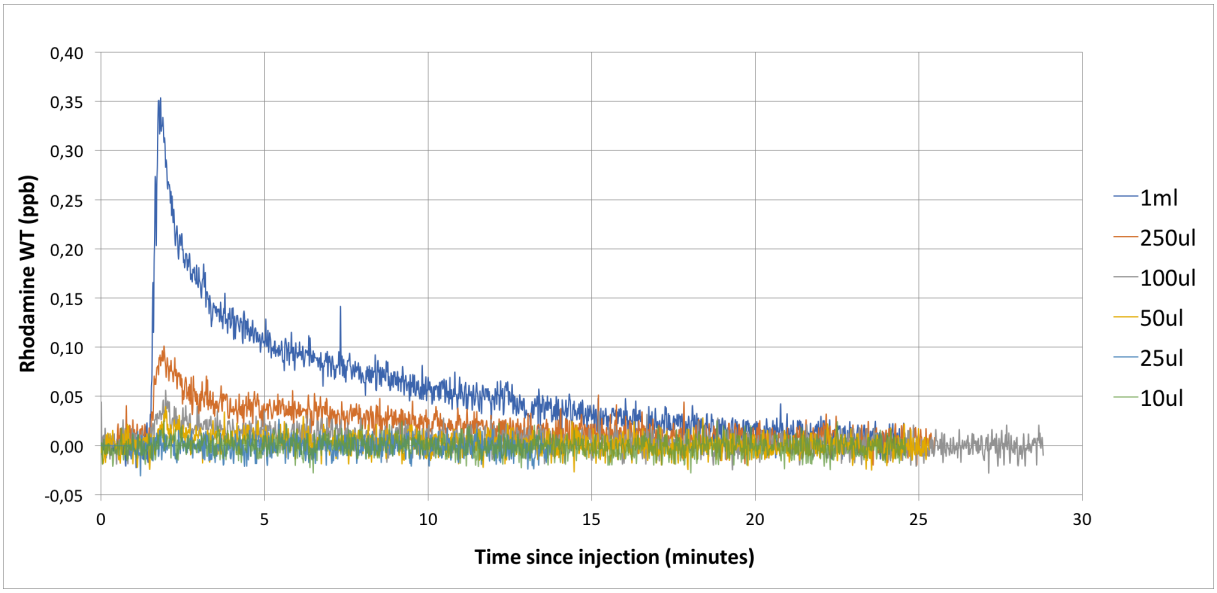

Figure 5.5 Breakthrough curves from Lab#15. Increasingly smaller volumes of Rhodamine WT were passed through a relatively large water volume until the signals were undetectable. The naming scheme indicates volumes of 1/50000 dilution of Rhodamine WT and water.

We performed measurements with 0,05µl injections of Rhodamine WT several times while changing different parameters, the results from this is shown in figure 5.6. Lab #13 was measured in the stream just below the injection, at Q = 7,89 L/min. Lab #14 was measured in the same place, but at a lower Q = 4,55 L/min. In Lab #15, the dye signal was also passed through a water volume containing 28 litres of water, before it was measured in an outlet stream below this at Q = 3,64 L/min. If we compare the breakthrough curves from Lab #14

and Lab #15 (before and after the water volume), the peak concentration in Lab #15 was reduced by 93,8%, and the curve was elongated to be 33 times longer.

The breakthrough curve from Lab #15(250) had an integrated volume larger than anticipated, resulting in an underestimation of the discharge (Q_E=2,72 L/min) which had been measured to be Q_A=3,64 L/min. Other measurements from Lab #15 also underestimated the flow, but to a lesser degree (Lab #15(1000) Q_E=3,12 L/min and Lab #15(100) Q_E=3,53 L/min). The large area under the curve in Lab #15(250) is interesting, because it is varying from the expected value by more than our instrumental error margins predict, in a controlled experiment. However, since this effect does not show up in the other, similar measurement (done with 0,2µl), the experiment would have to be repeated to see if the effect persists.

5.4.2 Valley lake signal distortion

Field measurement Lake #4 was done with the same dye volume and similar flow conditions as in Stream #2, but the signal was in addition passed through the valley lake. After going through the valley lake, the breakthrough curve's peak concentration was reduced by 91,8%, and the breakthrough curve was elongated to be 24 times longer, compared to Stream #2 (as shown in figure 5.7). The rough shape of the original breakthrough curve is still detectable, and it estimates the same discharge as Stream #2, which was performed during similar flow conditions.

5.4.3 Glacier lake signal distortion

In the field measurements Supra-stream #6 and Supra-lake #5, the signal from the supraglacial stream was passed through the glacial lake (figure 5.8). After going through the glacial lake, the breakthrough curve's peak concentration was reduced by 98,2%, and the breakthrough curve was elongated to be at least 35 times longer, compared to Supra-stream #6. The entirety of the draw-out tail was not measured, as the measurement had to be ended after 82 hours.

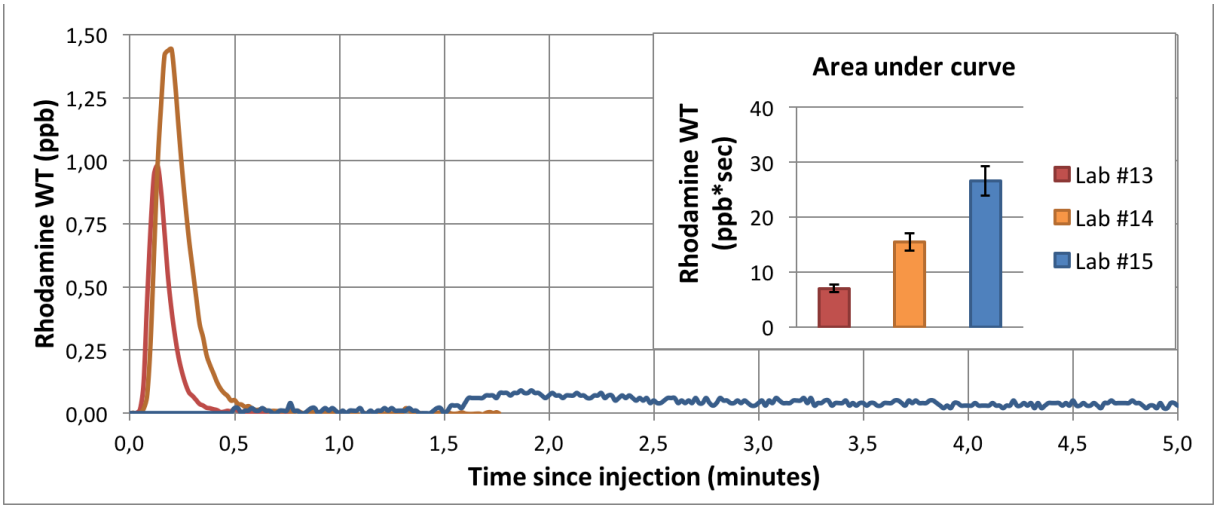

Figure 5.6 Breakthrough curves from three lab experiments done with 0,05µl Rhodamine WT with the same set up, although with varying discharges. Lab #15 has in addition been passed through a 28 litre water volume, which has reduced the peak concentration and stretched out the breakthrough curve.

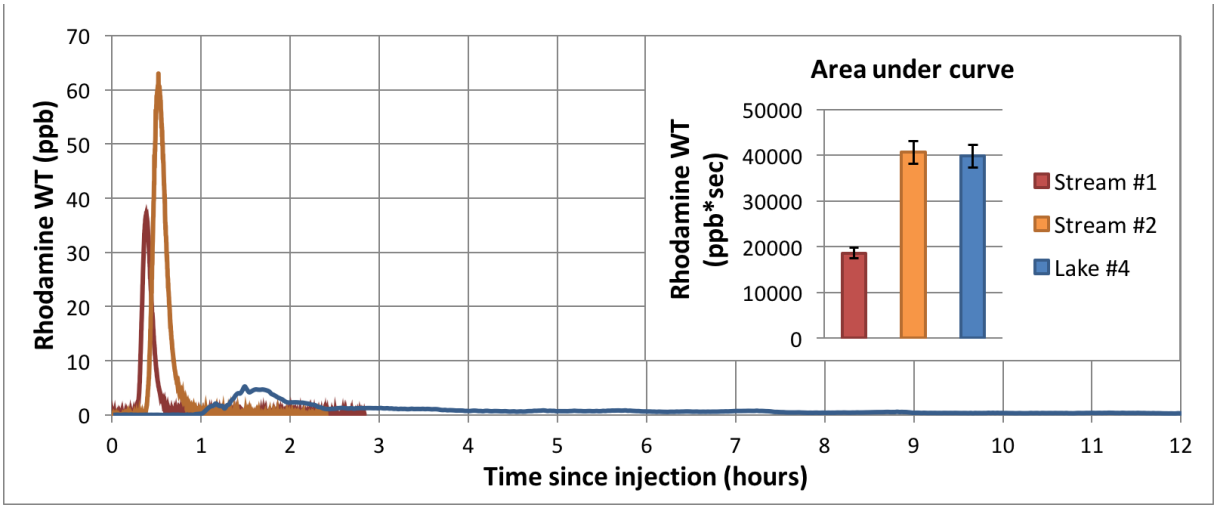

Figure 5.7 Breakthrough curves from three field measurements from the same rive in the Skjerdingane valley. Stream #1 and Stream #2 were done in the stream at different flow rates, and Lake #4 was in addition passed through the valley lake.

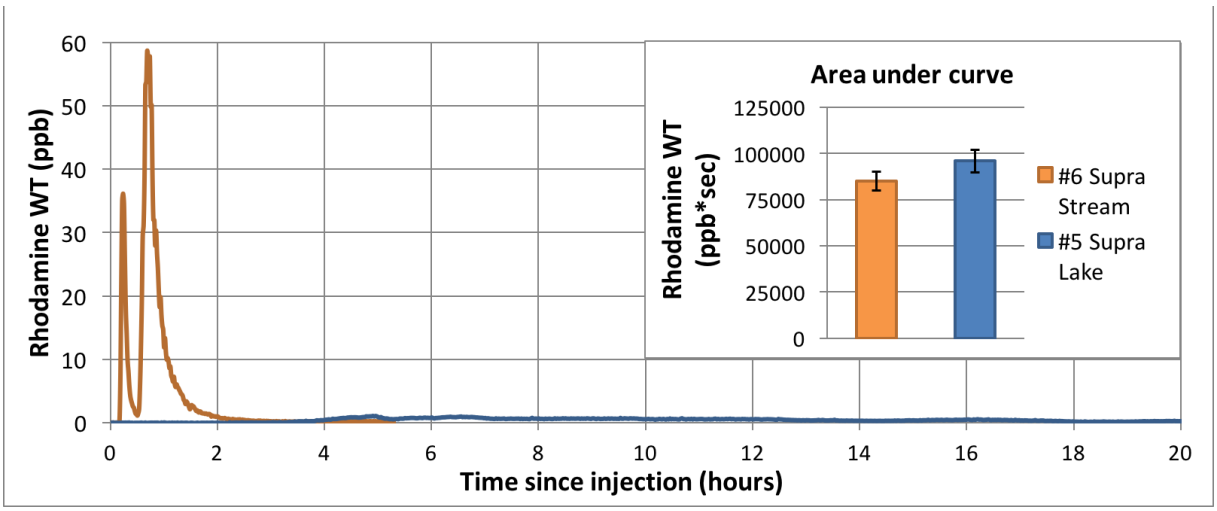

Figure 5.8 Breakthrough curves from the two field measurements done in the supraglacial stream. The stream measurement, Supra-stream #6, shows two distinct peaks. After being passed through the glacial lake, in Supra-lake #5, the peaks are no longer discernible.

The distinct double peak breakthrough curve from Supra-stream #6 is no longer recognizable in Supra-lake #5. The double peak represented an ideal signal for our test, as it is a strong and easily detectable signal, yet very simple. If not even this clear signal can be detected after being passed through the glacial lake, that indicates that other, more complex signals, will definitely not be detectable. Since the idea behind dye tracing is to analyse the breakthrough curves from dye clouds which have passed through the glacier, this result indicates that it would be very difficult to preserve even simple signals if they have to be passed through large water volumes.

Assuming that the glacial lake has a surface area of 5500 m^2 (estimated from aerial photos) and a mean depth of 1m, then the Q/volume is $5{,}09 \times 10^{-5}$ s^{-1}. Further assuming that the valley lake has a surface area of 7900 m^2 (estimated from aerial photos) and a mean depth of 1 metre, then the Q/volume for this lake is $3{,}58 \times 10^{-5}$ s^{-1}. In our lab experiment, Lab #15, the Q/volume was $2{,}16 \times 10^{-3}$ s^{-1}. The Q/volume for the two field lakes are fairly similar, while the lab experiment is not. If the lab experiment should be on the same order of magnitude, then the water volume would have to be increased from 28 litres to 2800 litres (or the flow would have to be reduced).

Figure 5.9 Overview image showing dye entering and spreading along the sides of the valley lake during field measurement Lake #4. Photo: Jan Hedges

5.4.4 Temperature effects

The signal passed through the valley lake (Lake #4) was preserved better than the signal passed through the glacial lake (Supra-lake #5). This could be due to the effect of water temperature on internal mixing. We visually observed both measurements for a while in the field, and viewed the way that the dye cloud entered the water bodies. When entering the proglacial lake, the dye cloud visibly dispersed down and into the lake, below the surface. In the valley lake, the dye cloud dispersed visibly along the edges of the lake, and stayed close to the surface (shown in figure 5.9).

These observations are not conclusive; for example, the dye could be spreading just as much down into the valley lake as along the surface, but the surface spread is clearly visible due to larger concentrations than in the glacial lake. Still, this could indicate that in the valley lake, the warmer, aeriated water from the mountain stream could float on top of the colder, denser water already present in the lake. This would allow it to take a more direct route to the outlet of the valley lake where the fluorometer was set up, than if it had had to disperse through the entire lake. Similarly, if the cold meltwater from the glacier was not able to float on top in this manner, that might partly explain why the signal from Supra-lake #5 was so much weaker than the signal from Lake #4.

5.4.5 Error sources

Whenever dye tracing is affected by a lake, there will be a large number of more or less unknown variables. The size of the lake will have a large effect on how the dye signal is affected, and lake sizes are hard to estimate, especially in a glacial environment. The internal geometry of the lake might have an effect, as would any internal circulation or lack thereof. The average temperature of the lake, as well as any internal variations in temperature, could affect the signal. The signal could also be affected by the amount and type of suspended sediment and the type of bedload sediment. The chemical composition of the lake could also affect the dye signal. An additional effect is that the lake is likely to receive inflow from other sources than just the water where the dye has been injected, which further complicates the result. This list is not exhaustive.

5.4.6 Further investigations

This preliminary investigation has highlighted many of the difficulties encountered when a large body of water is interfering with a dye trace study. Further work could include steps to develop a numerical model which could better simulate dispersion of dye through a 3D-

system. Refining and repeating lab experiments where dye signals are measured before and after being passed through water volumes in controlled conditions, could also lead to a better understanding of the process. Finally, gathering more data from the field and looking for patterns in how different types of lakes affect dye signals, could lead to a better understanding of how the process works in the real world.

6 Conclusion

In this thesis, we have used fluorometric dye tracing techniques to estimate the melt season discharge of the Skjerdingane cirque glacier. The reliability of these estimates has been tested in lab experiments and simulated with a numerical model. This process has also provided a better understanding of the theory and the methodology behind dye tracing techniques, which was one of the main goals of this project.

We have also shown that retrieving dye signals from the subglacial drainage system is difficult, in large part due to the interference from the proglacial lake. This raises the question of how much the glacial lake reduces the dye signal. A larger quantity of injected dye might be able to pass a detectable signal through the lake. Even then, we have shown that very distinct breakthrough curves can become unrecognizable after being passed through a lake. Further investigations are needed into how a dye breakthrough curve is affected by being passed through a large water volume.

7 References

Andreassen, L. M., Winsvold, S. H., Paul, F., & Hausberg, J. (2012). Inventory of Norwegian glaciers. *NVE, Oslo*.

Bencala, K. E., Rathbun, R. E., Jackman, A. P., Kennedy, V. C., Zellweger, G. W., & Avanzino, R. J. (1983). RHODAMINE WT DYE LOSSES IN A MOUNTAIN STREAM ENVIRONMENT1: Wiley Online Library.

Benn, D., & Evans, D. J. (2014). *Glaciers and glaciation*: Routledge.

Chapman, R. (2002). *Physics for geologists*: CRC Press.

Clark, D. B., Lenain, L., Feddersen, F., Boss, E., & Guza, R. (2014). Aerial imaging of fluorescent dye in the near shore. *Journal of Atmospheric and Oceanic Technology, 31*(6), 1410-1421.

Corporation, K. A. (2002). Keyacid rhodamine wt liquid. *Keystone Aniline R&D Labratories Technical Bulletin 89*.

Designs, T. Cyclops 7 data sheet.

Designs, T. Cyclops 7 Optical Specification Guide.

Designs, T. (2017, 11. April). [DataBank logging].

Falkovich, G. (2011). *Fluid mechanics: A short course for physicists*: Cambridge University Press.

Fountain, A. G. (1993). Geometry and flow conditions of subglacial water at South Cascade Glacier, Washington State, USA; an analysis of cracer injections. *Journal of Glaciology, 39*(131), 143-156.

Fyffe, C. L. (2013). Tracer investigations. *School of the Environment, University of Dundee*, 9.

Gendron, P.-O., Avaltroni, F., & Wilkinson, K. J. (2008). Diffusion Coefficients of Several Rhodamine Derivatives as Determined by Pulsed Field Gradient–Nuclear Magnetic Resonance and Fluorescence Correlation Spectroscopy. *Journal of Fluorescence, 18*(6), 1093. doi:10.1007/s10895-008-0357-7

Gulley, J., Walthard, P., Martin, J., Banwell, A., Benn, D., & Catania, G. (2012). Conduit roughness and dye-trace breakthrough curves: why slow velocity and high dispersivity may not reflect flow in distributed systems. *Journal of Glaciology, 58*(211), 915-925.

Hubbard, B., & Glasser, N. F. (2005). *Field techniques in glaciology and glacial geomorphology*: John Wiley & Sons.

Kartverket (Cartographer). WMS Ortofoto. Retrieved from http://wms.geonorge.no/skwms1/wms.nib?

Kartverket (Cartographer). WMS topografisk kart. Retrieved from http://wms.geonorge.no/skwms1/wms.topo2?

Kartverket (Cartographer). (2010). Areal Skjerdinganebreen Norgeskart [Flyfoto]. Retrieved from http://www.norgeskart.no/ -!?project=seeiendom&layers=1003,1014&zoom=13.94131994647273&lat=6827149.77&lon=62809.14&drawing=943273790887cce704d79309977a9f30072ed847

Kilpatrick, F. A., & Cobb, E. D. (1985). Measurement of Discharge Using Tracers.

Lau, M. A. (2016). Spreadsheet Implementation of Numerical and Analytical Solutions to Some Classical Partial Differential Equations. *Spreadsheets in Education (eJSiE), 9*(3), 1.

Nesje, A. (2012). *BRELÆRE bre, landskap, klimaendringer og datering 2.utgave* (Vol. 2): Høyskoleforlaget.

Nienow, P., Sharp, M., & Willis, I. (1998). Seasonal changes in the morphology of the subglacial drainage system, Haut Glacier d'Arolla, Switzerland. *Earth Surface Processes and Landforms, 23*(9), 825-843.

NVE. (2016a). Percipitation data, Selseng. Retrieved from http://www.xgeo.no/graphapp/index.html?X=69078&Y=6826739&searchT=10000&stationId=55730.0.1&app=xgeo&tab=meteogramAvalanche

NVE. (2016b). Temperature at Anestølen og Frudalen. Retrieved from http://www.xgeo.no/graphapp/index.html?X=66136&Y=6828580&searchT=10000&stationId=55735.17.1&app=xgeo

Piccolo, C. (2016). Using EXCEL Spreadsheets to Solve a 1D Heat Equation. 9.

Seaberg, S. Z., Seaberg, J. Z., Hooke, R. L., & Wiberg, D. W. (1988). Character of the englacial and subglacial drainage system in the lower part of the ablation area of Storglaciären, Sweden, as revealed by dye-trace studies. *Journal of Glaciology, 34*(117), 217-227.

Smart, P., & Laidlaw, I. (1977). An evaluation of some fluorescent dyes for water tracing. *Water resources research, 13*(1), 15-33.

Willis, I. C., Sharp, M. J., & Richards, K. S. (1990). Configuration of the drainage system of Midtdalsbreen, Norway, as indicated by dye-tracing experiments. *Journal of Glaciology, 36*(122), 89-101.

Wilson, J. F., Cobb, E. D., & Kilpatrick, F. A. (1968). *Fluorometric procedures for dye tracing*: US Government Printing Office.